THE PREVALENCE OF TRIMETHOPRIM-RESISTANCE-CONFERRING DIHYDROFOLATE REDUCTASE GENES IN MULTIDRUG RESISTANT BACTERIA FROM CLINICAL ISOLATES IN MALAYSIA

By

YU LEE WEN

A project report submitted to the Department of Allied Health Sciences

Faculty of Science

Universiti Tunku Abdul Rahman

in partial fulfilment of the requirements for the degree of

Bachelor of Science (Honours) Biomedical Science

May 2024

ABSTRACT

THE PREVALENCE OF TRIMETHOPRIM-RESISTANCE-CONFERRING DIHYDROFOLATE REDUCTASE GENES IN MULTIDRUG RESISTANT BACTERIA FROM CLINICAL ISOLATES IN MALAYSIA

YU LEE WEN

Antibiotic resistance has been a global issue since the appearance of drug-resistant microorganisms. With the limited medicines available, the treatment of bacterial infections is now at risk of failure. Trimethoprim is commonly used as a first- or second-line antibiotic in combination with sulfamethoxazole to treat uncomplicated urinary tract infections. However, the rising rate of antibiotic resistance renders this affordable drug ineffective. Gram-negative bacteria typically develop resistance to trimethoprim-sulfamethoxazole by gaining the *dfr* and *sul* genes, which are transferable between bacteria. The *dfr* genes are frequently found on the gene cassette located on the integron. The purpose of this study was to investigate the prevalence of *dfrA* genes in 60 clinical bacterial isolates, as well as their antimicrobial susceptibility to seven antibiotics from five classes: β-lactam combination agents, folate pathway antagonists, quinolones, aminoglycosides, and polymyxin. Triplex polymerase chain reaction (PCR) was performed to detect the presence of *dfrA* genes in total DNA extracted using the fast boil method. The susceptibility of the isolates was then determined using the Kirby-Bauer disc diffusion method. The

antimicrobial susceptibility data revealed that 76.67% of the bacterial isolates were resistant to amoxicillin-clavulanic acid, 70.00% to trimethoprim-sulfamethoxazole, 68.33% to ciprofloxacin, 61.67% to nalidixic acid, 18.33% to tobramycin, 8.33% to netillin, and 5.00% to polymyxin B. In triplex PCR, eight isolates were positive for *dfrA1* (13.33%), nine for *dfrA7* (15.00%), and none for *dfrA17*. Co-carriage of the *dfrA* genes was not seen. The *Chi*-square or Fisher's exact test was used to evaluate the association between the *dfrA* genes and trimethoprim-sulfamethoxazole resistance, as well as the patient's age and gender. The findings indicate that *dfrA7* was positively associated with ciprofloxacin and trimethoprim-sulfamethoxazole resistance. However, the patient's age and gender showed no significant association with the presence of *dfrA* genes.

ACKNOWLEDGEMENT

Foremost, I extend my deepest gratitude to Dr. Chew Choy Hoong, my supervisor, for her invaluable guidance, unwavering support, and constructive feedback throughout this research journey. Dr. Chew's expertise, encouragement, and patience have played a pivotal role in shaping the direction and refining the quality of this thesis.

I am sincerely thankful to the laboratory supervisors at UTAR, namely Ms. Fatin, Ms. Hemaroopini, and Mr. Saravanan, as well as the laboratory assistants, including Ms. Siti Nor Ain, Ms. Natrah, Mr. Mohd Zaini, Ms. Nur Izzati, and Ms. Nurfarhana, for providing the essential resources and a conducive environment for this study. A special acknowledgment goes to Mr. Wong Chi Hau, a postgraduate student, whose generous commitment in offering guidance and constructive advice significantly contributed to the completion of this project.

Additionally, I express my gratitude to my fellow lab mates, Andrew Yap Choo Yao, Grace Kong Kah Yi, Tan Jia Huey, and Yong Ker Shing, for their insightful comments and scientific contributions, which have enhanced the depth and content of this thesis. I am deeply thankful to my family for their unwavering love, encouragement, and understanding throughout this academic journey, serving as a constant source of motivation and inspiration. It is with their love and support that I became stronger.

DECLARATION

I hereby declare that this final year project is based on my original work except for quotations and citations which have been duly acknowledged. I also declare that it has not been previously or concurrently submitted for any other degree at UTAR or other institutions.

Yu Lee Wen

APPROVAL SHEET

This final year project report entitled "**THE PREVALENCE OF TRIMETHOPRIM-RESISTANCE-CONFERRING DIHYDROFOLATE REDUCTASE GENES IN MULTIDRUG RESISTANT BACTERIA FROM CLINICAL ISOLATES IN MALAYSIA**" was prepared by **YU LEE WEN** and submitted as partial fulfilment of the requirements for the degree of Bachelor of Science (Hons) Biomedical Science at Universiti Tunku Abdul Rahman.

Approved by:

Assoc. Prof Dr Chew Choy Hoong Date: 6th June 2024

Supervisor

Department of Biomedical Science

Faculty of Science

Universiti Tunku Abdul Rahman

FACULTY OF SCIENCE

UNIVERSITI TUNKU ABDUL RAHMAN

Date: 26th April 2024

PERMISSION SHEET

It is hereby certified that **YU LEE WEN** (ID No: **20ADB03382**) has completed this final year project thesis entitled "THE PREVALENCE OF TRIMETHOPRIM-RESISTANCE-CONFERRING DIHYDROFOLATE REDUCTASE GENES IN MULTIDRUG RESISTANT BACTERIA FROM CLINICAL ISOLATES IN MALAYSIA" under the supervision of Dr. Chew Choy Hoong (Supervisor) from Department of Allied Health Sciences, Faculty of Science.

I hereby give permission to the University to upload the softcopy of my final year project in pdf format into the UTAR Institutional Repository, which may be made accessible to the UTAR community and public.

Yours truly,

(YU LEE WEN)

TABLE OF CONTENTS

LIST OF TABLES

LIST OF FIGURES

LIST OF APPENDICES

LIST OF ABBREVIATIONS

A260	Absorbance at 260 nm
A260/A280 ratio	Nucleic acid purity ratio
A280	Absorbance at 280 nm
AMC	Amoxicillin-clavulanic acid
AMR	Antimicrobial resistance
bp	Base pair
CLSI	Clinical and Laboratory Standard Institute
COVID-19	Coronavirus disease 2019
DHFR	Dihydrofolate reductase
DNA	Deoxyribonucleic acid
dNTP	Deoxynucleoside triphosphate
EDTA	Ethylenediaminetetraacetic acid
F	Female
FPGS	Folylpoly-gamma-glutamate synthetase
I	Intermediately resistant
M	Male
MDR	Multidrug Resistant
$MgCl_2$	Magnesium chloride
min	Minutes
mM	Millimolar
ng	Nanogram
nm	Nanometre
PCR	Polymerase chain reaction

R	Resistant
RNA	Ribonucleic acid
rpm	Revolution per minute
S	Susceptible/Sensitive
TAE	Tris, acetic acid, EDTA
Taq	*Thermus aquaticus*
TMP-SMZ	Trimethoprim-sulfamethoxazole
TSA	Tryptic soy agar
u	Enzyme unit
UPEC	Uropathogenic *Escherichia coli*
UTI	Urinary tract infection
V	Volts
w/v	Weight per volume
µL	Microlitre
µM	Micromolar

CHAPTER 1

INTRODUCTION

The rapid emergence of antimicrobial resistance (AMR) among bacterial isolates, particularly Gram-negative bacteria, has become a public health crisis in the 21st century. The AMR leads to the ineffectiveness of the antibiotic drugs administered to the patient with a bacterial infection, causing an increased risk of mortality, the length of hospital stays, and the cost of health care. Several mechanisms of antibiotic resistance are involved in the development of AMR in bacteria. These include inhibition of drug absorption, alteration of drug targets, drug inactivation, and the use of efflux pumps. Multidrug resistance (MDR) is defined by Alkofide, et al. (2020) as the acquired resistance to one agent from three or more classes of antimicrobial agents. In addition, a pan-drug-resistant (PDR) infection is known to occur when the bacteria are resistant to all the currently used antimicrobial agents (Ozma, et al., 2022). A study conducted by Antimicrobial Resistance Collaborators (2022) estimated that bacterial AMR was associated with 4.95 million deaths. Furthermore, the rising rate of emergence of AMR bacteria is projected to cause up to 10 million casualties annually by 2050 (Somorin, et al., 2022).

Trimethoprim is a synthetic antimicrobial agent that was first described in 1962 and has been available for clinical use in combination with sulfamethoxazole in Europe since 1968 (Delanaye, et al., 2011). It is synthesised by Bushby and Hitchings as a sulfonamide potentiator (Zinner and Mayer, 2015).

Trimethoprim inhibits an enzyme that is important in the folate biosynthesis pathway, leading to the inhibition of DNA and purine base synthesis in bacteria.

Trimethoprim is a low-cost antibiotic extensively used in clinical settings to treat and prevent urinary tract infections (UTIs). The use of trimethoprim has been widespread in developing countries as a first-line drug due to its affordability (Huovinen, 2001). However, the rapid establishment and spread of trimethoprim resistance among clinical isolates has resulted in treatment failure. Currently, trimethoprim is only used when there is a low chance of resistance, as opposed to the preferred antibiotic, nitrofurantoin (Somorin, et al., 2022). Nevertheless, trimethoprim is still commonly used because of the high incidence of gastrointestinal side effects with nitrofurantoin and its contraindication in patients with poor renal function.

In Malaysia, patients are usually not prescribed trimethoprim for treatment of UTI, but instead, trimethoprim-sulfamethoxazole is being prescribed. It is worth noting that over one-third of the prescribed antibiotics for UTI consist of trimethoprim-sulfamethoxazole (Teng, et al., 2011). According to the Malaysian antibiotic guidelines report, there was an overall decrease in AMR in Gram-negative bacteria such as *Escherichia coli* and *Klebsiella pneumoniae* between 2013 and 2018. However, the resistance rate of trimethoprim-sulfamethoxazole in urine isolates of *E. coli* (36.4%) and *K. pneumoniae* (33.6%) in 2018 is still regarded as high when compared to the majority of the other antibiotics mentioned, such as amikacin (5.1%) and imipenem (3.1%) (Ministry of Health Malaysia, 2019).

Furthermore, there are only a limited number of cost-effective antimicrobial drugs available in clinical settings, so determining the resistance phenotypes of bacterial isolates before prescribing trimethoprim sulfamethoxazole is crucial to maintaining antibiotic efficacy. To address this major public health risk, a thorough understanding of the distribution of trimethoprim resistance conferring genes, or *dfrA*, among the clinical isolates is required. Therefore, the relationship between the trimethoprim-sulfamethoxazole resistance phenotype and the prevalence of the dihydrofolate reductase (*dfrA*) gene in clinical isolates must be investigated to prevent the emergence of more trimethoprim-sulfamethoxazole-resistant bacteria, which can render antibiotic treatment ineffective, as well as to prevent the bacteria from becoming resistant to other classes of useful antibiotics.

The objectives of this study are as follows:

a) To identify the antimicrobial susceptibility phenotypes of clinical isolates collected from hospitals in Malaysia.
b) To screen and detect the presence of *dfrA* genes (*dfrA1*, *dfrA7*, and *dfrA17*) in the clinical isolates via triplex polymerase chain reaction (PCR).
c) To investigate the prevalence of *dfrA* genes (*dfrA1*, *dfrA7*, and *dfrA17*) in clinical bacterial isolates.
d) To analyse the association between *dfrA* gene prevalence and antimicrobial resistance phenotypes, as well as patient demographic profiles such as age and gender.

CHAPTER 2

LITERATURE REVIEW

2.1 Antibacterial Antifolates

2.1.1 Overview

Antifolates work by interfering with the folate cycle, which is centred on the folate molecule. Folate refers to tetrahydrofolate and its derivatives. Folate is an essential component of several metabolic activities that support key biological functions, including amino acid metabolism, mitochondrial tRNA modification, methyl group biosynthesis, and nucleic acid synthesis (Engelking, 2015; Zheng and Cantley, 2018). Naturally occurring folates include tetrahydrofolate and dihydrofolate.

Tetrahydrofolate and dihydrofolate differ in the oxidation state of their pterine rings, with dihydrofolate being the oxidised form that requires dihydrofolate reductase (DHFR) to be reduced to tetrahydrofolate. Tetrahydrofolate is an active cofactor in the folate pathway, which promotes the production of nucleic acids and amino acids. Tetrahydrofolate consists of a pterine ring, a para-aminobenzoic acid (PABA) moiety, and an L-glutamate moiety (Figure 2.1). The tetrahydrofolate molecules consist of a single carbon unit with different oxidation states attached to the N5 and/or N10 positions (Figure 2.1). The tetrahydrofolate molecule has been observed to undergo several minor modifications and has approximately 150 members (Fernández-Villa, Aguilar, and Rojo, 2019).

A

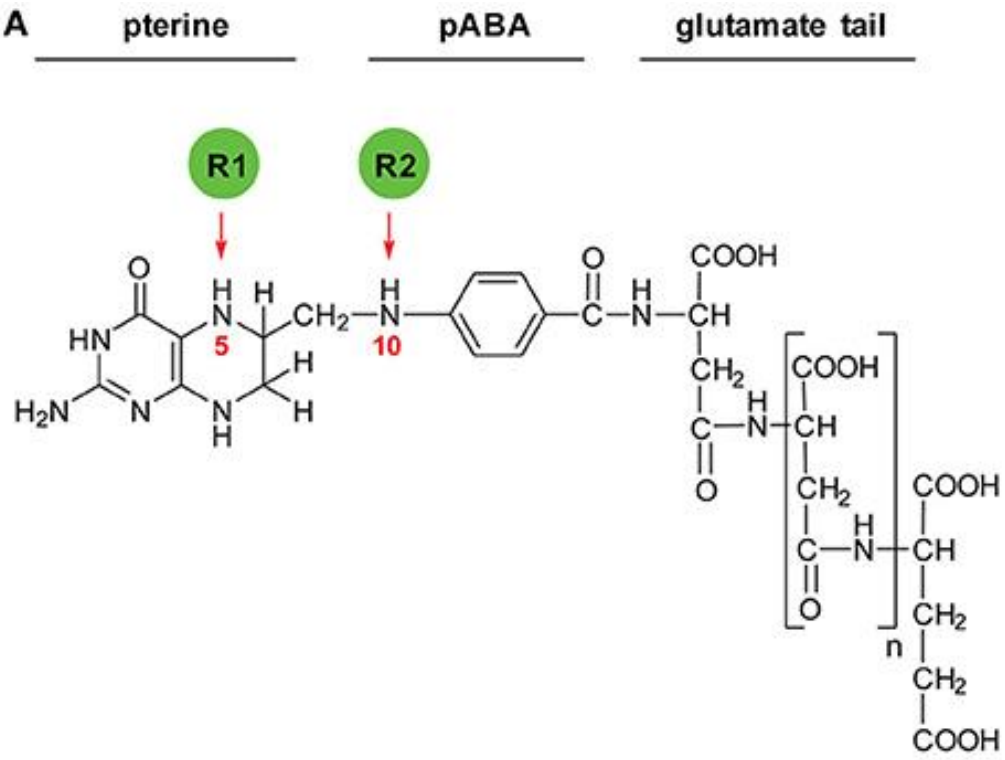

B

Folate species	R1 (N5)	R2 (N10)
Tetrahydrofolate (THF)	-H	-H
5-methyl THF	$-CH_3$	-H
5,10-methylene THF	$-CH_2-$	$-CH_2$
5,10-methenyl THF	$-CH=N^+$	$-CH=N^+$
5-formyl THF	-CHO	-H
10-formyl THF	-H	-CHO
10-formimino THF	-H	-CHNH

Figure 2.1: Molecular structure of tetrahydrofolate and its derivatives (Adapted from Gorelova, et al., 2017).

(A) Chemical structure of the tetrahydrofolate molecule. R1 and R2 represent the various one-carbon units, while red arrows indicate their positions. (B) One-carbon substituents that are carried by the tetrahydrofolate.

There are two types of antifolates based on their chemical structures: classical and non-classical antifolates (Figure 2.2). Classical antifolates are structural analogues of folate and interfere with the folate production pathway by competing with the enzyme involved in folate metabolism. In terms of chemical structure, classical inhibitors consist of a heterocyclic ring attached to the aryl group and a glutamate tail. The non-classical antifolates, on the other hand, are structurally different from folate to the target enzyme, which is missing in humans, and provide selectivity against bacterial cells but not mammalian cells. The non-classical antifolates have lipophilic side chains and can enter cells by passive diffusion. They have been developed to overcome resistance to classical inhibitors (Wróbel, et al., 2019).

The differences in the folate pathway between humans and bacteria are known, allowing the use of non-classical antifolates against bacteria for the treatment of infections. Bacteria, protozoa, plants and unicellular eukaryotes can synthesise folate *de novo* using enzymes such as dihydrofolate reductase (DHFR), however higher eukaryotic species such as humans cannot synthesise folate *de novo* but can receive sufficient folate from their diet. In addition, bacteria cannot absorb folate and its derivatives due to the absence of the folate receptor on their cell membranes. Bacteria must therefore synthesise their own folate *de novo* to maintain essential metabolic functions. This divergence in the folate biosynthetic pathway between bacteria and humans highlighted the pioneering strategy to combat bacterial infections in the 1930s (Fernández-Villa, Aguilar, and Rojo, 2019). Furthermore, folic acid is a synthetic folate that must be reduced twice to produce active folate.

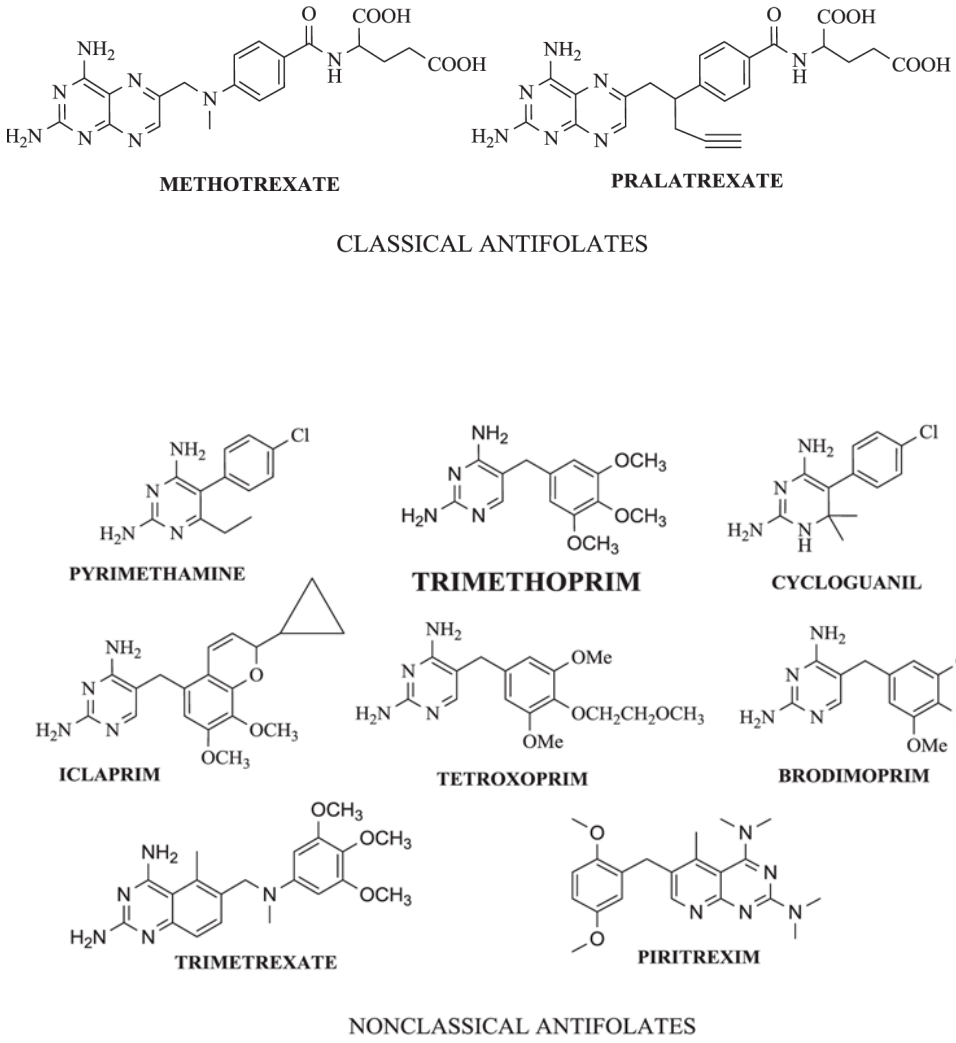

Figure 2.2: Chemical structures of classical and non-classical antifolates (Adapted from Wróbel, et al., 2019).

2.1.2 Mechanism of Action of Trimethoprim in Folate Pathway

The folate pathway involves several enzymes that are crucial for various metabolic processes necessary for cell function and survival (Figure 2.3). One of these enzymes is DHFR, which converts 5,6-dihydrofolic acid (DHF) to its active form, 5,6,7,8-tetrahydrofolic acid (THF), in the presence of the cofactor nicotinamide adenine dinucleotide phosphate (NADPH). When trimethoprim interacts with DHFR, hydrogen bonds are established between the protonated

aminopyrimidine group of the drug and the enzyme's carboxylate group, resulting in the formation of a specific hydrogen-bonded ring motif. DHFR is a central enzyme in the folate pathway, which is crucial for the maintenance of the folate cycle (Fernández-Villa, Aguilar, and Rojo, 2019). Trimethoprim inhibits the DHFR enzyme, leading to disruption of the folate pathway.

In addition, THF and its derivatives are the key precursor molecules required for one-carbon transfer processes and for the biosynthesis of DNA nitrogenous bases and amino acids (Manna, et al., 2021). Trimethoprim interferes with the conversion of DHF to THF, ultimately leading to an imbalance in the folate pathway that inhibits the synthesis of thymidylate and purine bases. This is followed by inhibition of bacterial DNA synthesis and cell death. Trimethoprim is an antibiotic that exhibits broad-spectrum activity and is capable of either inhibiting bacterial growth (bacteriostatic) or causing bacterial cell death (bactericidal) against a diverse array of Gram-positive and Gram-negative bacteria. However, it typically lacks effectiveness against anaerobic bacteria. (Hismiogullari and Yarsan, 2009).

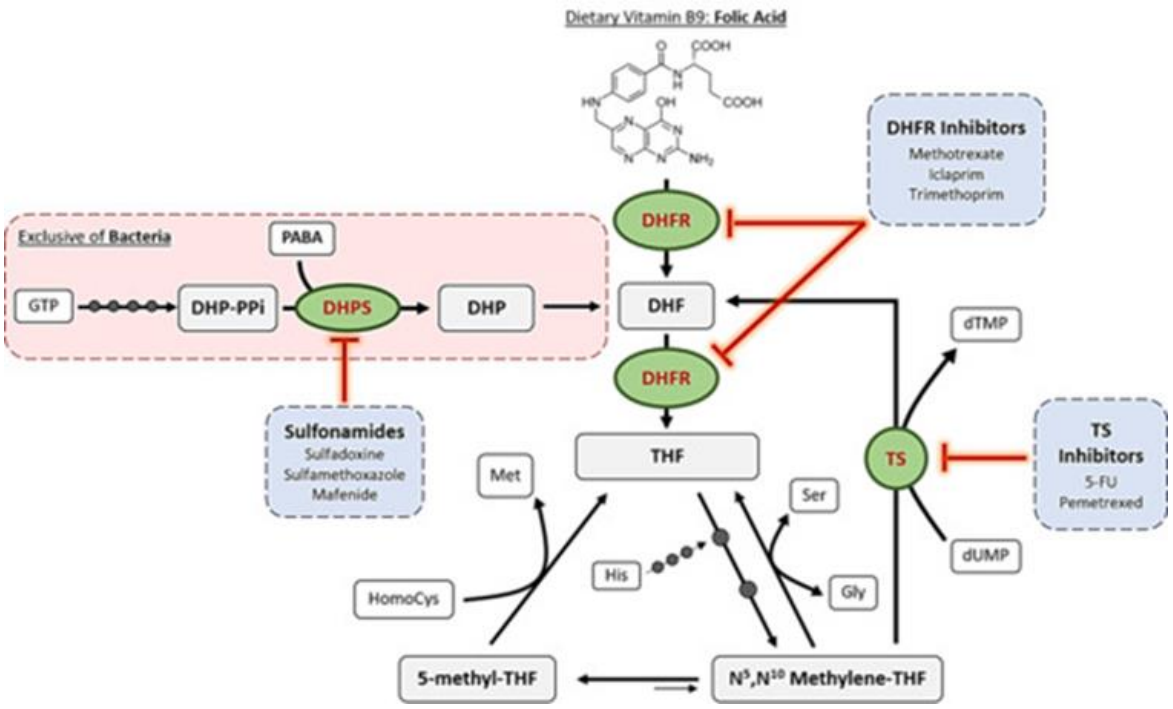

Figure 2.3: The principal enzymes involved in the folic acid pathway and therapeutic compounds used to inhibit them (Adapted from Fernández-Villa, Aguilar and Rojo, 2019).

DHP: dihydropteroate; **DHP-PPi:** dihydropteroate pyrophosphate; **DHPS:** dihydropteroate synthase; **DHF:** dihydrofolate; **DHFR:** dihydrofolate reductase; **Gly:** glycine; **GTP:** guanosine triphosphate; **His:** histidine; **HomoCys:** homocysteine; **Met:** methionine; **PABA:** p-aminobenzoic acid; **Ser:** serine; **THF:** tetrahydrofolate, and **TS:** thymidylate synthase.

2.2 Trimethoprim Antibiotics

2.2.1 Molecular Structure of Trimethoprim

Trimethoprim, 5-[(3,4,5-trimethoxyphenyl) methyl]pyrimidine-2,4-diamine, is a synthetic antibacterial drug from the class of diaminopyrimidines (Wróbel, et al., 2019). It consists of pyrimidine-2,4-diamine and 1,2,3-trimethoxybenzene linked by a methylene bridge, as depicted in Figure 2.4 (EMBL's European Bioinformatics Institute, 2017). According to X-ray crystallographic studies by Matthews, et al. (1985), trimethoprim does not bind to the nucleotide-binding site of the mammalian DHFR enzyme but fits well into the homologous site of the bacterial enzyme. As a result, trimethoprim has high selectivity for the bacterial DHFR enzyme, allowing it to be used as an antimicrobial agent. Hismiogullari and Yarsan (2009) found that the bacterial enzyme is 20–60 times more susceptible to trimethoprim than the mammalian enzymes.

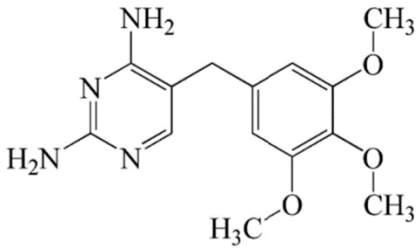

Figure 2.4: Molecular structure of trimethoprim (Adapted from Shehdeh Jodeh, et al., 2022).

2.2.2 Metabolism Pathway of Trimethoprim

The trimethoprim drugs are well absorbed into the blood and then distributed to the tissue via the blood stream. Following that, the metabolism of trimethoprim

is mainly carried out in the liver. Figure 2.5 shows that trimethoprim undergoes oxidative metabolism, primarily forming demethylated 3' and 4' metabolites. Other than that, its minor products consist of N-oxide metabolites and, to a lesser extent, benzylic metabolites. The enzymes CYP2C9 and CYP3A4 are mainly involved in the biotransformation of trimethoprim, with CYP1A2 having a minor role. The majority of the ingested trimethoprim is excreted unmodified in the urine. The parent drug is considered the therapeutically active form (DrugBank, 2022).

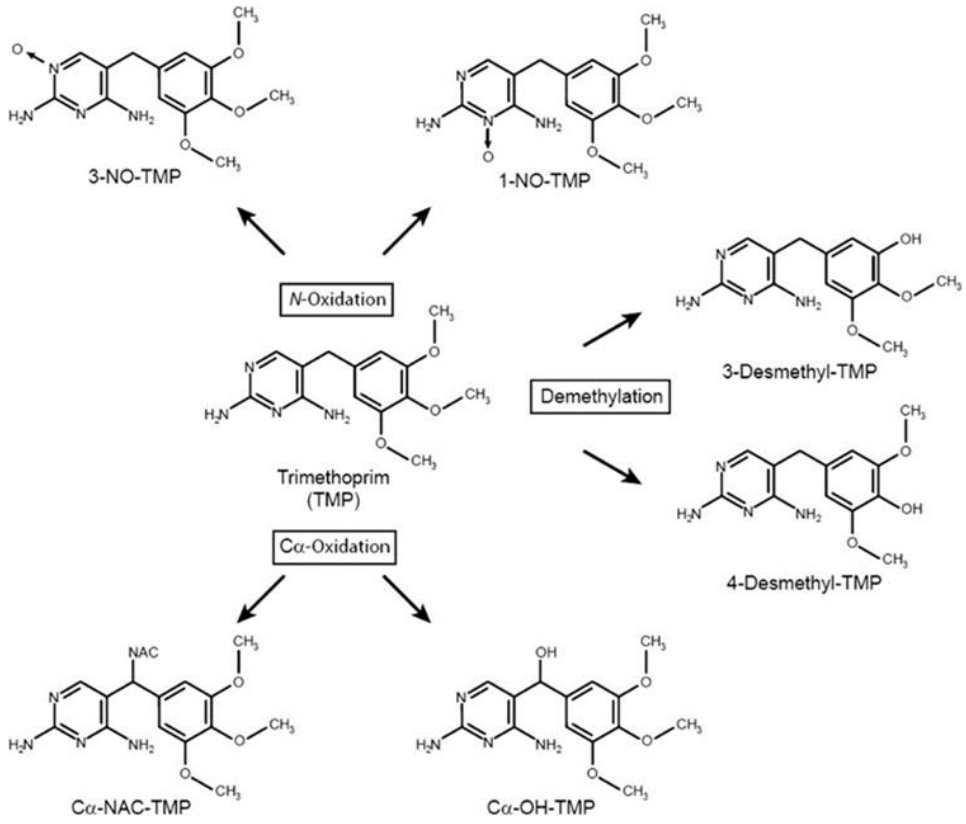

Figure 2.5: Metabolism pathways of trimethoprim to its primary metabolites (Adapted from Goldman, et al., 2015).

1-NO-TMP: TMP 1-N-oxide; **3-NO-TMP:** 3-N-oxide; **3′- and 4′-desmethyl-TMP**, C**α-OH-TMP:** benzylic alcohol, and **Cα-NAC-TMP:** N-acetyl cysteine TMP adduct.

2.2.3 Clinical Usage of Trimethoprim

Trimethoprim is an inexpensive and efficient antifolate antibiotic used in clinical settings to treat several forms of bacterial infections, particularly uncomplicated urinary tract infections (UTIs) such as cystitis in women. Various aetiological agents may contribute to UTIs, including *Enterobacteriaceae* species such as *E. coli* and *Klebsiella* species. Trimethoprim can be used alone or in combination with sulfamethoxazole to treat respiratory, enteric, and skin ailments. Although trimethoprim can be used alone to limit bacterial growth, the synergistic impact of trimethoprim-sulfamethoxazole will strengthen the inhibition of folate metabolism, whereby they both inhibit successive steps in folate synthesis in bacteria. Thus, the available preparation of trimethoprim-sulfamethoxazole with a 1:5 ratio is to attain the appropriate serum concentration, which enhances the bacteriostatic and bactericidal effects (Masters, et al., 2003). In the clinical setting, trimethoprim was first used in 1962 to treat *Proteus septicemia* along with sulphonamide and polymyxin (Wróbel, et al., 2019). Trimethoprim has also shown antifungal properties, where it can inhibit the *Candida albicans* DHFR (caDHFR) enzyme by acting as a competitive inhibitor (Wróbel, et al., 2019).

The extensive use of trimethoprim in the clinical setting has caused AMR to grow quickly, which makes treating infections more difficult. Furthermore, trimethoprim has been shown to be active against a number of malaria strains caused by *Plasmodium falciparum* (Wróbel, et al., 2019). Nonetheless, the limited effectiveness of trimethoprim against malaria was once again brought on by the establishment of resistance. Overall, the incidence of resistance

highlights the significance of prudent antibiotic usage and continuous research into alternative treatments, even if trimethoprim remains a mainstay in the treatment of some bacterial and fungal infections.

2.3 Resistance Mechanism Towards Antifolates

2.3.1 Overview

Various resistance mechanisms towards antifolates have been discovered. Figure 2.6 illustrates the mechanisms involved in bacterial resistance to antifolate antimicrobial agents. One common resistance mechanism is the acquisition of mutations within the gene responsible for encoding the targeted enzyme, such as DHFR, which reduces the binding ability of antifolates (Fernández-Villa, Aguilar and Rojo, 2019; Kordus and Baughn, 2019). Secondly, the emergence of a novel resistant isoform of the targeted enzyme by the antifolates, and thirdly, the reduced cell permeability and increased expression of efflux proteins for the antifolates (Fernández-Villa, Aguilar and Rojo, 2019). Alterations in the transport proteins of antifolates, including the influx and efflux transporters, cause decreased uptake or increased efflux of the antifolates, which enhances the development of antifolate resistance in cells. The overexpression of the targeted enzyme can cause deregulation of the folate pathway, resulting in resistance to antifolates.

Additionally, the deregulation of polyglutamylation by folylpoly-gamma-glutamate synthetase (FPGS) can contribute to antifolate resistance. Reduced expression of FPGS or decreased enzymatic activity can also contribute to antifolate resistance, as polyglutamylation of classical antifolates is crucial for

their intracellular retention and cytotoxicity. Finally, some microorganisms have a thymine auxotrophy, which means they require external sources of dTMP because of thymidylate synthase (TS) dysfunction (Fernández-Villa, Aguilar and Rojo, 2019). Figure 2.6 depicts the resistance mechanism against the antifolates.

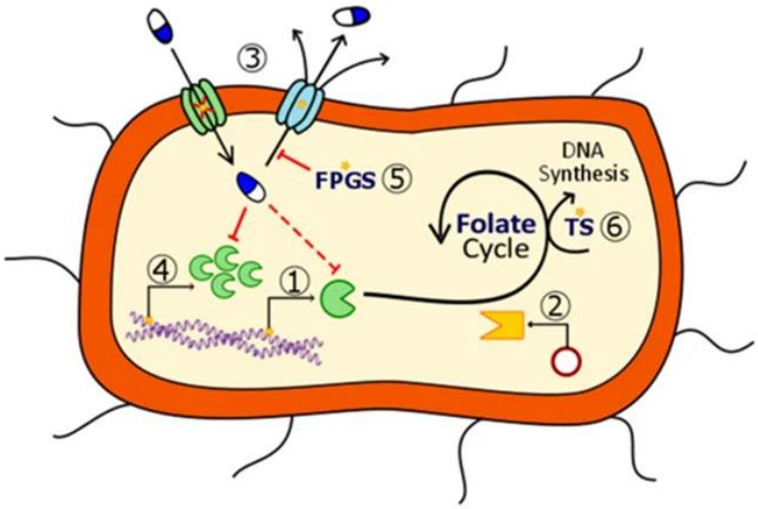

Figure 2.6: Resistance mechanisms against antifolates (Adapted from Fernández-Villa, Aguilar and Rojo, 2019).

2.4 Resistance to Trimethoprim

2.4.1 Overview

Trimethoprim resistance in bacteria can be either acquired or intrinsic. Intrinsic resistance is a characteristic commonly found across bacterial species that is not influenced by prior exposure to antibiotics and is not associated with horizontal gene transfer (HGT). Acquired resistance is due to genetic changes or the acquisition of genetic material that confers resistance to the antibiotic trimethoprim (Reygaert, 2018). The intrinsic mechanism of bacterial resistance

involves reduced outer cell membrane permeability. AMR genes can be acquired through horizontal gene transfer (HGT) mechanisms such as transformation, transposition, and conjugation (Reygaert, 2018). Plasmid-mediated transmission of antibiotic resistance genes is particularly common.

2.4.2 Intrinsic Resistance to Trimethoprim

Chromosomal resistance to trimethoprim can be attributed to the loss of thymidylate synthase activity, resulting in abundant DHFR activity, as bacteria can use an external source of thymine supply. Next, structural changes in the bacteria's porins can affect their susceptibility to trimethoprim. The chromosomal *folA* gene mutation in bacteria, which encodes for the DHFR enzyme, can confer trimethoprim resistance to bacteria by reducing the affinity of the drug for the enzyme and decreasing enzymatic inhibition. In addition, mutational changes in the *folA* gene promoter can lead to overproduction of the DHFR enzyme, increasing the bacteria's insusceptibility to trimethoprim (Grape, 2006).

At the mechanistic level, bacteria can exhibit intrinsic resistance to trimethoprim through four main antimicrobial mechanisms: limiting drug uptake, reduced binding affinity of the target protein, the ability to use the exogenous preformed folates, and actively effluxing drugs. For example, *Pseudomonas aeruginosa* exhibits resistance to trimethoprim due to reduced drug uptake. The resistance to trimethoprim in some other bacterial species, such as *Acinetobacter baumannii* and *Stenotrophomonas maltophilia*, is caused by the decreased binding affinity of the host DHFR enzyme to the drug

(Rossolini, Arena and Giani, 2017). Köhler, et al. (1996) showed that *P. aeruginosa* possesses a multidrug efflux system responsible for its intrinsic resistance to trimethoprim and sulfamethoxazole (SMX), which is the mexABoprM multidrug efflux system. Besides, *Enterococci*'s ability to utilise the exogenous folates has reduced its susceptibility to trimethoprim.

2.4.3 Acquired Resistance to Trimethoprim

Acquired trimethoprim resistance can be linked to DHFR overproduction induced by promoter mutations as well as mutations in the DHFR structural genes. For example, a mutation in the chromosomal DHFR gene (*dfrB*) at the promoter region may contribute to trimethoprim resistance, resulting in overproduction of the host DHFR enzyme. These mutations are frequently related to providing high-level resistance in *Enterobacteriaceae* bacteria. As a result, higher trimethoprim concentrations are needed to inhibit host cells.

However, it has been discovered that the principal mechanism for acquired trimethoprim resistance in enterobacteria is the acquisition of foreign genes (*dfrA*). The *dfrA* genes encode a trimethoprim resistant DHFR enzyme with an altered active site. This makes the antifolate-targeted enzyme resistant to inhibition by the trimethoprim antibiotic. The *dfrA* genes are frequently located on integron gene cassettes, allowing for the transmission of mobile trimethoprim resistance genes between bacterial isolates, resulting in high-level trimethoprim resistance (Grape, et al., 2007; Rossolini, Arena, and Giani, 2017).

2.5 Trimethoprim Resistance-Conferring (*dfr*) Genes

2.5.1 Trimethoprim Resistance Gene Families and Naming Convention

The genes responsible for trimethoprim resistance are divided into two families: *dfrA* and *dfrB*. This classification is based on evolutionary relationships and sequence similarities (Grape, et al., 2007; Sánchez-Osuna, et al., 2020). The *dfr* genes encode proteins that are evolutionarily unrelated and have widely varying sizes. The gene sequence similarity indicates that the *dfrA* gene is homologous to the chromosomally expressed *folA* gene found in bacterial isolates, whereas the *dfrB* gene is a functional analogue of unknown origin. The *dfrA* genes are normally named in accordance with a standard convention that includes the letters '*dfrA*' followed by an Arabic number denoting their discovery order. However, the *dfr* genes discovered in Gram-positive bacteria were previously assumed to be unrelated to those studied in Gram-negative bacteria. As a result, they were given the alphabetical names *dfrC-K* (Sánchez-Osuna, et al., 2020).

The *dfrA* genes are longer (at least 474 bases) than the *dfrB* genes (237 bases). According to van Hoek, et al. (2011), six plasmid-mediated *dfr* families have been found, with some of the *dfr* determinants originally coming from Gram-positive bacteria (*dfrC*, *dfrD*, *dfrG*, and *dfrK*), as indicated in Table 2.1. The majority of *dfr* genes were assigned to the first phylogenetic group, with over thirty members in the *dfrA* gene family and only roughly eight in the *dfrB* gene family. The genes in the *dfrA* gene family have a sequence similarity of roughly 20–95% when compared to one another and to other housekeeping genes; further classification of the genes into their subfamily of genes indicates a higher degree of relatedness (Grape, et al., 2007). The *dfrA1* group consists of

twelve distinct genes that share 64–90% amino acid identity; the *dfrA12* group, which consists of five members, has an amino acid identity of 84%. The extra *dfr* genes have a reduced amino acid sequence identity of less than 25% (Grape, et al., 2007; Sánchez-Osuna, et al., 2020).

2.5.2 Prevalence of *dfr* genes among Clinical Bacterial Isolates

The five most prevalent *dfr* genes determined in the bacterial isolates are *dfrA1*, *dfrA5*, *dfrA7*, *dfrA12*, and also *dfrA17* (Grape, et al., 2007; Somorin, et al., 2022). Notably, two of them (*dfrA1* and *dfrA17*) were found to be the predominant genes found in the clinical bacterial isolates studied in many regions, such as Portugal, Lithuana, and Sweden (Grape, et al., 2007; Brolund, et al., 2010; Šeputienė, et al., 2010; Amador, et al., 2019). Although these five common integron-carried trimethoprim resistance determinants are found to be widely spread worldwide, their prevalence varies across different geographical areas. In a study in Sweden, *dfrA1* was determined to be the most common trimethoprim resistance conferring gene among the *E. coli* isolates (34.00%) and *K. pneumoniae* isolates (15.00%), followed by *dfrA17* (26.00% in *E. coli*) in a study in Sweden (Brolund, et al., 2010). In another study in Kuwait, *dfrA7* and *17* (71.00%) genes were detected to have a higher prevalence than *dfrA1* (20.00%) in the trimethoprim-resistant population, which was then followed by *dfrA5* (17.00%) (Alajmi, Alfouzan and Mustafa, 2023). In Australia, there is a higher number of *dfrA17* (9.00%) positive isolates than *dfrA1* (0.00%) positive isolates (White, McIver, and Rawlinson, 2001).

2.5.3 Multidrug Resistance

As depicted in Figure 2.7, the *dfrA* genes are frequently linked to other antibiotic resistance genes (ARGs), which can provide bacteria with resistance to various antimicrobials. The *dfrA* genes confer resistance to trimethoprim, but they are often present in mobile genetic elements (MGEs), like plasmids or integrons of classes 1 or 2. These MGEs can carry multiple antibiotic resistance genes, enabling the simultaneous transfer of resistance to trimethoprim and other antibiotics between bacterial strains via horizontal gene transfer (HGT). Therefore, bacteria can develop and spread MDR. The *dfrA* gene can confer resistance in bacterial isolates to antibiotics other than trimethoprim, thus increasing the risk of antibiotic treatment failure for bacterial infections. For example, Al-Marzooq, Mohd Yusof and Tay (2015) stated that the majority of *K. pneumoniae* isolates in their study possessed several antibiotic resistance determinants including the *dfrA* genes and were resistant to various antibiotics. According to Kneis, et al. (2023), the *dfrA* genes were often discovered near other antimicrobial resistance genes, including *ant* and *aadA*, that confer resistance to aminoglycosides.

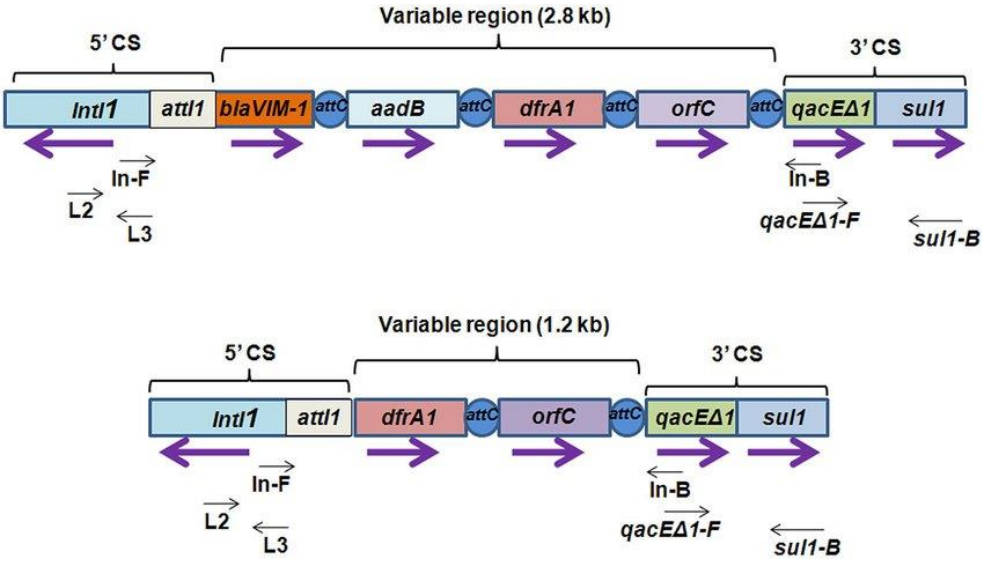

Figure 2.7: Schematic representation of class 1 integron harbouring gene cassettes with *dfrA1* and *sul1* genes (Adapted from Rajpara, et al., 2015).

Table 2.1: List of acquired trimethoprim resistance genes (van Hoek, et al., 2011).

Gene	Sub-family	Gene(s) included	Length (nt)	Accession number	Coding region	Genera
dfrA1	*dfrA1*-group	*dhfrIb, dfr1, dhfrI*	474	X00926	236..709	*Actinobacter, Enterobacter, Escherichia, Klebsiella, Morganella, Proteus, Pseudomonas, Salmonella, Serratia, Shigella, Vibrio*
dfrA3			489	J03306	103..591	*Salmonella*
dfrA5	*dfrA1*-group	*dhfrV, dfrV*	474	X12868	1306..1779	*Aeromonas, Enterobacter, Escherichia, Klebsiella, Salmonella, Vibrio*
dfrA6	*dfrA1*-group	*dfrVI*	474	Z86002	336..809	*Escherichia, Proteus, Vibrio*
dfrA7	*dfrA1*-group	*dhfrVII, dfrVII, dfrA17*	474	X58425	594..1067	*Actinobacter, Escherichia, Proteus, Salmonella, Shigella*
dfrA8			510	U10186	711..1220	*Shigella*
dfrA9			534	X57730	726..1259	*Escherichia*
dfrA10			564	L06418	5494..6057	*Actinobacter, Escherichia, Klebsiella, Salmonella*
dfrA12	*dfrA12*-group	*dhfrXII, dfr12*	498	Z21672	310..807	*Actinobacter, Aeromonas, Enterobacter, Enterococcus, Citrobacter, Klebsiella, Pseudomonas, Serratia, Salmonella, Staphylococcus*
dfrA13	*dfrA12*-group		498	Z50802	718..1215	*Escherichia*

Table 2.1 (continue):

dfrA14	*dfrA1*-group	*dhfrIb*	474	Z50805	72..545	*Achromobacter*, *Aeromonas*, *Escherichia*, *Klebsiella*, *Salmonella*, *Vibrio*
dfrA15	*dfrA1*-group	*dhfrXVb*	474	Z83311	357..830	*Enterobacter*, *Klebsiella*, *Morganella*, *Proteus*, *Pseudomonas*, *Salmonella*, *Vibrio*
dfrA16	*dfrA1*-group	*dhfrXVI*, *dfr16*	474	AF077008	115..588	*Aeromonas*, *Escherichia*, *Salmonella*
dfrA17	*dfrA1*-group	*dhfrXVII*, *dfr17*	474	AB126604	98..571	*Actinobacter*, *Enterobacter*, *Klebsiella*, *Pseudomonas*, *Salmonella*, *Serratia*, *Shigella*, *Staphylococcus*
dfrA18		*dfrA19*	570	AJ310778	7004..7573	*Enterobacter*, *Klebsiella*, *Salmonella*
dfrA20			510	AJ605332	1304..1813	*Pasteurella*
dfrA21	*dfrA12*-group	*dfrxiii*	498	AY552589	1..498	*Klebsiella*, *Salmonella*
dfrA22	*dfrA12*-group	*dfr22*, *dfr23*	498	AJ628423	325..822	*Escherichia*, *Klebsiella*
dfrA23			561	AJ746361	6743..7303	*Salmonella*
dfrA24			558	AJ972619	83..640	*Escherichia*
dfrA25	*dfrA1*-group		459	DQ267940	54..512	*Citrobacter*, *Salmonella*
dfrA26			552	AM403715	303..854	*Escherichia*
dfrA27	*dfrA1*-group	*dfr*	474	EU675686	2543..3016	*Escherichia*
dfrA28	*dfrA1*-group		474	FM877476	116..589	*Aeromonas*
dfrA29		*dfrVII*, *dfrA7*	472	AM237806	615..1086	*Salmonella*
dfrA30		*dhfrV*	474	AM997279	705..1178	unknown

Table 2.1 (continue):

dfrA31		*dfr6*	474	AB200915	1832..2305	*Vibrio*
dfrA32	*dfrA1*-group		474	GU067642	535..1008	*Laribacter*, *Salmonella*
dfrA33	*dfrA12*-group		498	FM957884	88..585	Unknown
dfrB1		*dhfrIIa*, *dfr2a*	237	U36276	717..953	*Aeromonas*, *Bordetella*, *Escherichia*, *Klebsiella*
dfrB2		*dhfrIIb*, *dfr2b*	237	J01773	809..1045	*Escherichia*
dfrB3		*dhfrIIc*, *dfr2c*	237	X72585	5957..6193	*Aeromonas*, *Enterobacter*, *Escherichia*, *Klebsiella*
dfrB4		*dfr2d*	237	AJ429132	69..305	*Aeromonas*, *Escherichia*, *Klebsiella*
dfrB5		*dfr2e*	237	AY943084	2856..3092	*Pseudomonas*
dfrB6			237	DQ274503	394..630	*Salmonella*
dfrB7			237	DQ993182	244..480	*Aeromonas*
dfrB8			249	GU295656	1048..1296	*Aeromonas*
dfrC		*dfrA*	486	Z48233	337..822	*Staphylococcus*
dfrD			489	Z50141	94..582	*Listeria*, *Staphylococcus*
dfrG			498	AB205645	1013..1510	*Enterococcus*, *Staphylococcus*
dfrK			492	FM207105	2788..3279	*Staphylococcus*

CHAPTER 3

MATERIALS AND METHODS

3.1 Chemicals and Reagents

Table 3.1 lists the chemicals and reagents utilised in this study, as well as their manufacturers and countries of origin.

Table 3.1: List of chemicals and reagents utilised, with their manufacturer and country of origin.

Chemicals and reagents	Manufacturer, Country of origin
Tryptic soy agar (TSA)	Merck KGaA, Germany
Mueller-Hinton agar	Himedia Laboratories Pvt. Ltd., India
Luria-Bertani (LB) broth	Condalab, Spain
Nutrient broth	Himedia Laboratories Pvt. Ltd., India
Agarose powder	1st Base Laboratories, Singapore
Trimethoprim-sulfamethoxazole (TMP-SMZ), ciprofloxacin antibiotic discs	Oxoid Group Holdings Limited, United Kingdom
Amoxicillin-clavulanic acid, nalidixic acid antibiotic discs	Liofilchem S.r.l., Italy
Netillin, tobramycin, polymyxin B antibiotic discs	Himedia Laboratories Pvt. Ltd., India

Table 3.1 (continue):

Chemicals and reagents	Manufacturer, Country of origin
5X Green GoTaq® Flexi Buffer	Promega Corporation, United States of America
GoTaq® G2 Flexi DNA Polymerase	Promega Corporation, United States of America
Forward and reverse primers	Integrated DNA Technologies Pte. Ltd., Singapore
50 bp DNA ladder RTU	GeneDireX, Inc., United States of America
Novel Juice	GeneDireX, Inc., United States of America
Deoxynucleotide triphosphates (dNTP) mix	Promega Corporation, United States of America
Magnesium chloride ($MgCl_2$)	Promega Corporation, United States of America
Tris base	Vivantis Technologies Sdn. Bhd., Malaysia
Glacial acetic acid	QRëC™, New Zealand
EDTA disodium salt	Grupo RNM, Portugal

3.2 Bacterial Samples Collection

Multidrug-resistant bacterial isolates were collected from various hospitals in Malaysia, including Innoquest Pathology (formerly known as Gribbles

Pathology) (Ipoh, Kuala Lumpur, Penang, and Seremban), Hospital Pantai (Ipoh), KPJ Ipoh Specialist Hospital (Ipoh), and Hospital Raja Permaisuri Bainun (Ipoh). Following ethical approval from the Medical Research and Ethics Committee, the samples were collected and stored as glycerol stock at -80°C. This study documented the gender, age, and types of specimens obtained from the patient (Appendix A). This study included 60 multidrug-resistant bacterial isolates, mostly from the *Enterobacteriaceae* family, comprising eight different species: 31 *Klebsiella pneumoniae*, 17 *Escherichia coli*, three *Enterobacter cloacae*, one isolate for each of the bacterial species *Morganella morganii*, *Enterobacter amnigenus*, *Enterobacter aerogenes*, *Citrobacter freundii*, and lastly, five *Pseudomonas aeruginosa* isolates were also included.

3.3 Bacterial Culture

The bacterial samples were revived from glycerol stocks by streaking them on tryptic soy agar (TSA) plate. After inoculation of the agar plates, the plates were incubated at 37°C for overnight. The revived samples were kept at 4°C for further analysis and testing.

3.4 Antimicrobial Susceptibility Test

The antimicrobial susceptibility test was conducted out utilising the Kirby-Bauer disc diffusion method. To obtain the McFarland standard turbidity of 0.5, one or two colonies of the bacterial isolate were taken from the pure bacterial culture using an inoculation loop and inoculated into 5 ml of 0.85% sterile normal saline solution (LaPierre, et al., 2020). The turbidity of the inoculated bacterial suspension was then contrasted with the 0.5 McFarland standard

(Biomerieux) on a white background including dark horizontal lines to aid in comparison. To remove any excess water, the sterile cotton swab was pressed up against the test tube wall after being dipped into the bacterial mixture. The inoculum was spread evenly by streaking the inoculated cotton swab across the plate. The agar plate was then left to dry for 3–5 minutes.

Seven types of antibiotics were used to treat the bacterial isolates: amoxicillin-clavulanic acid (30 µg), trimethoprim-sulfamethoxazole (TMP-SMZ) (25 µg), nalidixic acid (30 µg), ciprofloxacin (5 µg), netillin (30 µg), tobramycin (10 µg), and polymyxin B (300 µg). The antibiotic discs were gently pressed into the dried agar plate with sterile forceps to ensure proper contact with the surface of the agar. The agar plates were incubated for approximately 16–18 hours at 37°C. The bacterial isolates' resistance phenotypes were categorised as resistant (R), intermediate (I), or sensitive (S) using the Clinical & Laboratory Standards Institute (CLSI) interpretative categories and inhibitory zone diameter breakpoints. In addition, interpretative breakpoints provided by Mehrishi, et al. (2019) and Al-Ajmi, Rahman, and Banu (2020) were considered for classification (Appendix B). The diameter of the inhibition zone in millimetres was measured to determine the classification. To ensure quality control, *Escherichia coli* ATCC 25922 was used as the reference strain.

3.5 Total DNA Extraction

The total DNA was prepared using the fast boil method as described by Kor, Choo, and Chew (2013). A single bacterial colony was inoculated from the master culture plate and placed in 5 ml of sterile nutrient broth. The bacterial

broth suspension was aerobically cultured for 24 hours in a shaking incubator set at 37°C and 220 rpm. Following that, 1.5 ml of the bacterial broth culture was aliquoted to a sterile 1.5 ml microcentrifuge tube. The bacterial broth culture was centrifuged at 12000 rpm for about 5 minutes, with the supernatant discarded. The bacterial pellet was resuspended in 300 µl of sterile distilled water using a vortex mixer. The suspensions were boiled at 100 °C using a heat block for 5 minutes, then immediately incubated on ice for the subsequent 2 minutes. The sample was centrifuged again at 12000 rpm for another 2 minutes, and the supernatant containing the total DNA was transferred to a new sterile 1.5 ml microcentrifuge tube. The Thermo Scientific™ Nanodrop™ 2000/2000c Spectrophotometer was used to analyse the concentration and purity of extracted DNA samples based on their absorbance ratio (A260/A280). DNA samples with an A260/A280 ratio ranging from 1.8 to 2.0 were considered pure, whereas those outside of this range were re-extracted. The DNA samples were kept at -20°C for further testing.

3.6 Optimisation of Duplex PCR

In this study, the optimisation of the duplex PCR conditions for detecting *dfrA1* and *dfrA7* genes was done. Gradient PCR was performed with different annealing temperatures ranging from 53.9°C to 70.0°C to determine the optimal annealing temperature for amplifying specific amplicons and minimizing the occurrence of non-specific bands.

3.7 Multiplex Polymerase Chain Reaction

Tables 3.2 and 3.3 list the cycling conditions and components used in the preparation of the PCR master mix. Prior to the PCR, the concentration of DNA for each bacterial isolate was adjusted to a standardised level of 100 µg/nl. Table 3.4 includes the primer sequences for detecting the three targeted trimethoprim resistance-conferring genes (*dfrA1*, *dfrA7*, and *dfrA17*) along with their expected product size. The PCR reactions were carried out using the Biometra T-Personal 48 Thermocycler.

Table 3.2: Cycling conditions for the triplex PCR (Grape, et al., 2007).

Stages	Temperature (°C)	Duration (s)	Number of cycles
Initial denaturation	95	600	1
Denaturation	94	45	
Annealing	60	45	30
Extension	72	120	
Final extension	72	600	1
Hold	4	∞	-

Table 3.3: Components of the PCR master mix for a single reaction (Grape, et al., 2007).

PCR reaction components	Initial concentration	Final concentration	Volume (µl)
5X Green GoTaq® Flexi Reaction Buffer	5X	1X	5.00

Table 3.3 (continue):

$MgCl_2$	25 mM	2.5 mM	2.50
dNTP	10 mM	0.2 mM	0.50
dfr1-f	10 µM	0.5 µM	1.25
dfr1-r	10 µM	0.5 µM	1.25
dfr7&17-f	10 µM	1.0 µM	2.50
dfr7-r	10 µM	0.5 µM	1.25
dfr17-r	10 µM	0.5 µM	1.25
GoTaq® G2 Flexi DNA Polymerase	5 u/µl	0.6 u	0.12
Sterile deionised water, ddH_2O	-	-	8.38
DNA template	-	100 µg/nl	1
Total volume	-	-	25

Table 3.4: Primer sequences and expected product sizes for detecting *dfrA1*, *dfrA7*, and *dfrA17* genes.

Gene	**Sequences (5' to 3')**	**Size (bp)**	**Citation**
dfrA1	F: TGGTAGCTATATCGAAGAATGGAGT	425	(Grape, et al., 2007).
	R: TATGTTAGAGGCGAAGTCTTGGGTA		
dfrA7	F: ACATTTGACTCTATGGGTGTTCTTC	227	
	R: ACCTCAACGTGAACAGTAGACAAAT		
dfrA17	F: ACATTTGACTCTATGGGTGTTCTTC	171	
	R: TCTCTGGCGGGGGTCAAATCTAT		

3.8 Agarose Gel Electrophoresis

Gel electrophoresis was used to examine the amplified PCR products. To serve as the running buffer, the 5X TAE buffer solution was diluted into the 1X with sterile deionised water. Table 3.5 lists the reagents and its amounts used to prepare the 10X TAE stock buffer solution. The GeneDireX 50 bp DNA Ladder RTU (Ready-to-Use) was employed as a molecular size marker to interpret the band sizes of the PCR products obtained. Five µl of DNA ladder and each of the PCR products were mixed with 1 µl of novel juice and loaded into the wells. The PCR products were electrophoresed at 80V for 40 minutes on a 3.0% (w/v) agarose gel. After that, the gel was examined using the Molecular Imager® Gel DocTM XR System (Bio-Rad).

Table 3.5: Components and amounts used in the 1L 10X TAE buffer preparation (Sigma Aldrich, 2021).

Components	Amount (g)
Tris base	48.5
Glacial acetic acid	11.4
0.5 M EDTA (pH 8.0)	20

3.9 Statistical Analysis

The software IBM® SPSS® Statistics 29.0.2.0 (20) was used to compile and analyse the data collected for this study in order to ascertain whether the prevalence of *dfrA1* and *dfrA7* and the antimicrobial susceptibility profile, as well as patient demographic profiles like age group and gender, are statistically significantly correlated by using the *Chi*-square analysis or Fisher's exact test.

The statistical tests were only performed on the *dfrA1* and *dfrA7* genes, as the *dfrA17* gene was lacking in all clinical isolates. A *p*-value of less than 0.05 indicates a significant correlation.

CHAPTER 4

RESULTS

4.1 Overview

The study successfully revived 60 clinical isolates. The eight bacterial species revived were *Klebsiella pneumoniae*, *Escherichia coli*, *Enterobacter cloacae*, *Morganella morganii*, *Enterobacter amnigenus*, *Enterobacter aerogenes*, *Citrobacter freundii*, and *Pseudomonas aeruginosa*. Table 3 in Appendix A summarises the demographic information for each clinical isolate.

The *Chi*-square test or Fisher's exact test was used to analyse the association between resistance phenotypes to trimethoprim-sulfamethoxazole (TMP-SMZ) and the trimethoprim resistance conferring gene (*dfrA*). Resistance to TMP-SMZ antibiotics is conferred by both the *dfr* (trimethoprim resistance gene) and *sul* (sulfonamide resistance gene) genes. Phenotypic and genotypic profiles of antimicrobial susceptibility were obtained using the Kirby-Bauer disc diffusion test and simultaneous detection of the *dfrA* gene in clinical isolates by multiplex PCR. Three TMP resistance genes (*dfrA1*, *dfrA7,* and *dfrA17*) were screened. Based on the Kirby-Bauer disc diffusion test, 70.00% (n = 42) of the bacterial isolates were identified as TMP-SMZ-resistant strains. Of the 42 bacterial isolates resistant to TMP-SMZ, 8 (19.05%) were positive for *dfrA1*, 9 (21.43%) were positive for *dfrA7,* and none of the isolates were found to contain *dfrA17*. It is also noteworthy that none of the isolates contained all three genes (*dfrA1*, *dfrA7,* and *dfrA17*) simultaneously.

4.2 Demographic Profiles of Clinical Isolates

In this study, demographic parameters such as the gender of the patient and their age group were used to correlate with the distribution of the target genes, the *dfrA* genes. The distribution of clinical isolates based on the gender and age groups of the patients is shown in Figure 4.1. There are three categories of age groups included in this study. The patients aged between 0 and 14 years are the young age group, and the working age group is defined as those aged between 15 and 64 years (Organisation for Economic Co-operation and Development, 2024). However, in this study, the maximum age of the working age group is set at 59 years old because 60 years old is the maximum retirement age in Malaysia, as stated in the "Minimum Retirement Age Act 2012" in the Laws of Malaysia. Thus, patients aged 60 years and older are considered to be in the old age group. Overall, there is a higher prevalence of older (≥60 years old) males (60.00%) in the samples examined in this study.

(a)

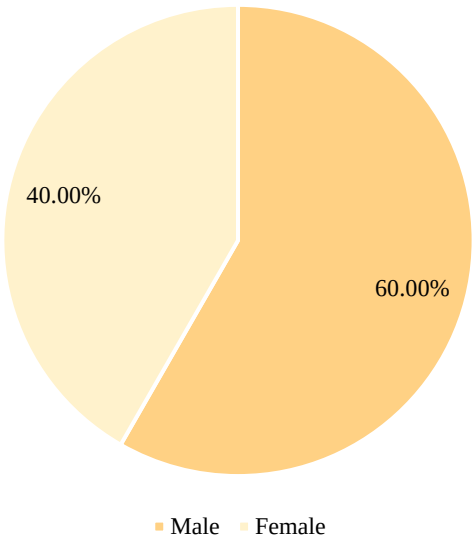

(b)

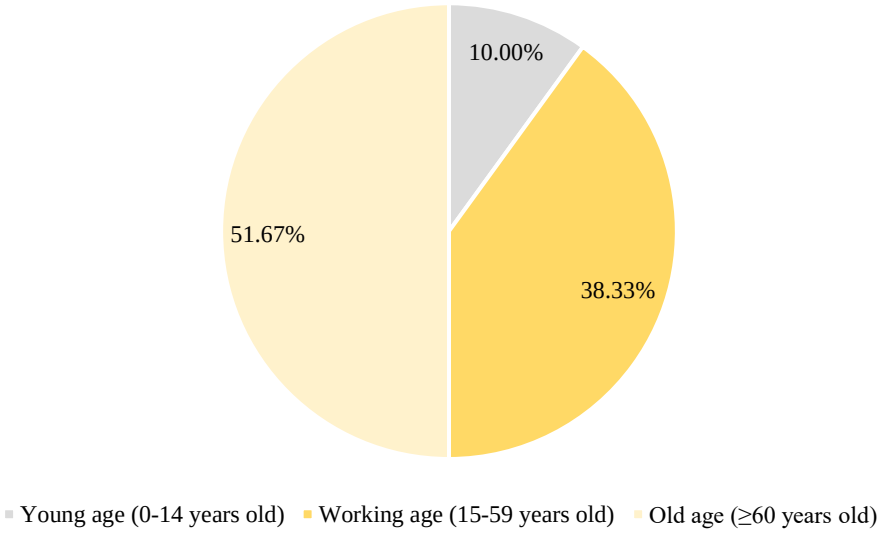

Figure 4.1: Gender and age group distribution of clinical isolates.

(a) The distribution of clinical isolates by gender. (b) Distribution of clinical isolates by age group.

4.3 Antimicrobial Susceptibility Profile

Clinical isolates were tested for susceptibility to seven types of antibiotics, including β-lactam combination agents (amoxicillin-clavulanic acid), folate pathway antagonists (trimethoprim-sulfamethoxazole (TMP-SMZ)), quinolones (nalidixic acid, ciprofloxacin), aminoglycosides (netillin, tobramycin), and polymyxin (polymyxin B). Results were interpreted according to CLSI guidelines and interpretative breakpoints provided by Mehrishi, et al. (2019) and Al-Ajmi, Rahman and Banu (2020) (Appendix B). The diameter of the inhibition zone was measured in millimetres to determine susceptibility to each antibiotic. For ease of analysis, isolates classified as 'intermediate' were grouped with 'resistant' in the phenotyping of the antimicrobial susceptibility profile and interpreted as such (Table 4.1). Figure 4.2 shows the representative image for the antimicrobial susceptibility test using the Kirby-Bauer disc diffusion method, where each isolate was treated with seven types of antibiotics. The isolates were shown to be resistant when an absence or small zone of inhibition formed around the antibiotic disc.

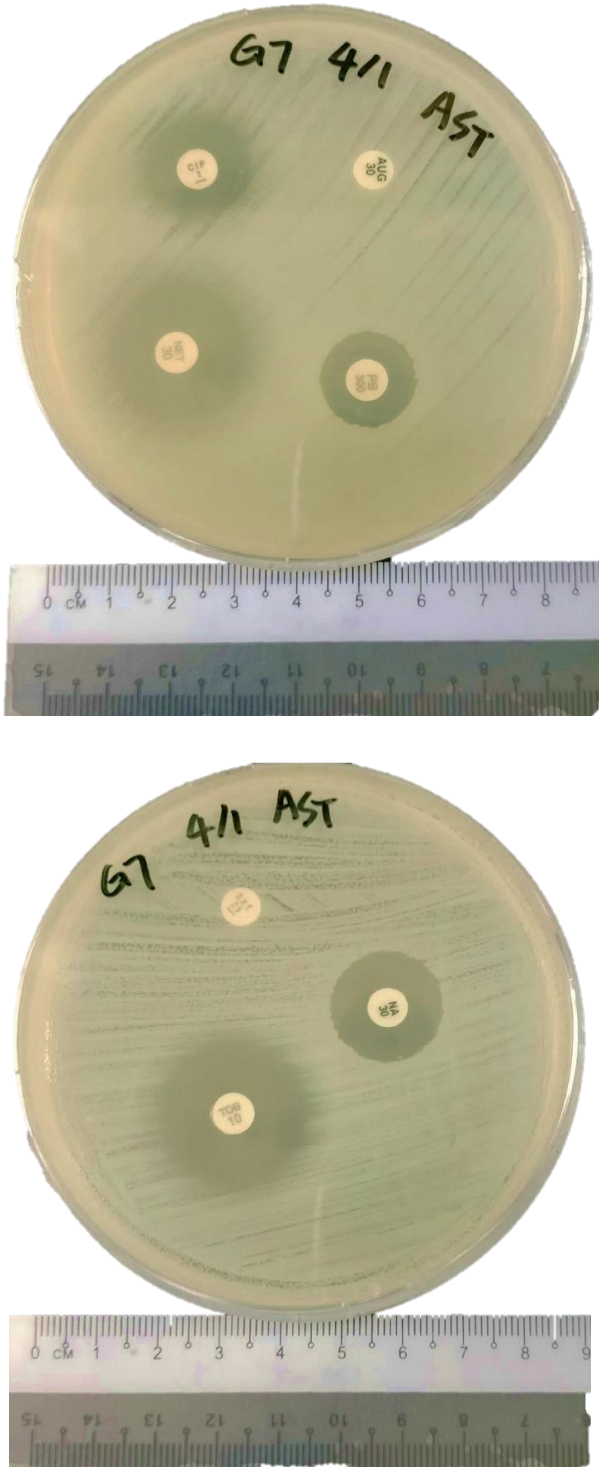

Figure 4.2: Representative images for antimicrobial susceptibility testing (Kirby-Bauer disc diffusion method).

TMP-SMZ: trimethoprim-sulfamethoxazole (25 µg); **AMC**: amoxicillin-clavulanic acid (30 µg), **NA**: nalidixic acid (30 µg), **NET**: netillin (30 µg), **CIP**: ciprofloxacin (5 µg), **TOB**: tobramycin (10 µg), and **PB**: polymyxin B (300 µg). The G7 strain of *E. coli* displayed resistance to ciprofloxacin (16 mm), amoxicillin-clavulanic acid (0 mm), and trimethoprim-sulfamethoxazole (0 mm). It also showed intermediate resistance to nalidixic acid (17 mm) and susceptibility to netillin (21 mm) and tobramycin (23 mm).

Of the 55 clinical *Enterobacteriaceae* isolates, 49 (89.09%) were resistant to at least one of the antibiotics tested, while the remaining six isolates (10.91%) were susceptible to all antibiotics tested. These isolates cannot be interpreted as non-MDR strains, as they may be associated with other antibiotic resistances not included in this study. Furthermore, the current edition of CLSI (2024) guidelines does not provide interpretive categories for the antibiotics nalidixic acid, amoxicillin-clavulanic acid, and polymyxin B when used against *Pseudomonas aeruginosa*. Consequently, the AST profile for these antibiotics is interpreted based on the breakpoints provided by CLSI (2011) and Mehrishi, et al. (2019) for *P. aeruginosa*.

Figure 4.3 shows that clinical isolates had the highest resistance rate to amoxicillin-clavulanic acid (76.67%), followed by trimethoprim-sulfamethoxazole (TMP-SMZ) (70.00%), ciprofloxacin (68.33%), nalidixic acid (61.67%), tobramycin (18.33%), netillin (8.33%), and finally polymyxin B (5.00%). On the other hand, *P. aeruginosa* showed the highest rate of resistance to trimethoprim-sulfamethoxazole (100.00%), amoxicillin-clavulanic acid (60.00%), followed by ciprofloxacin (40.00%), while none of the isolates were resistant to netillin, tobramycin or polymyxin B. The current CLSI guidelines only include the microdilution method as the sole method for analysis of polymyxin B antibiotic susceptibility for *Enterobacteriaceae* and *P. aeruginosa* bacterial isolates. Accordingly, the study evaluated the antimicrobial resistance phenotypes of polymyxin B in *Enterobacteriaceae* using a breakpoint category presented by Al-Ajmi, Rahman, and Banu (2020).

Table 4.1: Phenotypic antimicrobial resistance profiles of clinical isolates.

Species	Isolates	TOB	PB	NET	CIP	AMC	TMP-SMZ	NA
Escherichia coli	A7	S	S	S	R	R	R	R
Enterobacter cloacae	G21	R	S	S	R	R	S	R
Morganella morganii	G52	S	S	S	S	S	S	S
Citrobacter freundii	G63	S	S	S	R	R	R	R
Enterobacter aerogenes	G66	S	S	S	S	S	S	S
Enterobacter cloacae	G69	S	S	S	R	R	R	R
Escherichia coli	G7	S	S	S	R	R	R	R
Escherichia coli	H12	R	S	S	R	R	R	R
Klebsiella pneumoniae	H14	R	S	R	R	R	S	R
Klebsiella pneumoniae	H15	S	S	S	R	R	R	R
Klebsiella pneumoniae	H16	S	S	S	S	S	S	S
Klebsiella pneumoniae	H19	S	S	S	S	S	S	S
Escherichia coli	H21	S	S	S	R	R	R	R
Klebsiella pneumoniae	H22	S	S	S	S	S	S	R
Enterobacter amnigenus	H23	S	S	S	S	R	S	S
Klebsiella pneumoniae	H26	S	S	S	R	R	R	R
Klebsiella pneumoniae	H27	S	S	S	S	S	S	R
Klebsiella pneumoniae	H28	S	S	S	R	R	R	R
Escherichia coli	H3	R	R	R	R	S	S	R
Klebsiella pneumoniae	H31	R	S	S	R	R	R	R
Klebsiella pneumoniae	H32	S	S	S	R	R	R	R
Escherichia coli	H33	S	S	S	S	R	R	S
Klebsiella pneumoniae	H34	S	S	S	S	S	S	S

Table 4.1 (continue):

Escherichia coli	H35	S	S	S	R	R	R	R
Klebsiella pneumoniae	H38	R	S	R	R	R	R	R
Klebsiella pneumoniae	H4	R	S	R	R	R	S	R
Klebsiella pneumoniae	H40	S	S	S	R	R	R	S
Escherichia coli	H41	S	S	S	R	R	R	R
Klebsiella pneumoniae	H43	R	S	S	R	R	R	R
Klebsiella pneumoniae	H45	S	S	S	R	R	R	R
Enterobacter cloacae	H5	S	S	S	R	R	R	R
Escherichia coli	H52	S	S	S	R	R	R	R
Escherichia coli	H54	S	S	S	R	R	R	R
Klebsiella pneumoniae	H55	S	S	S	R	R	R	R
Klebsiella pneumoniae	H56	S	R	S	S	S	S	S
Klebsiella pneumoniae	H57	S	S	S	S	S	S	R
Klebsiella pneumoniae	H58	S	S	S	R	R	R	R
Escherichia coli	H59	S	S	S	R	R	R	S
Klebsiella pneumoniae	H6	S	S	S	R	R	R	R
Klebsiella pneumoniae	H62	S	S	S	S	R	R	S
Klebsiella pneumoniae	H63	R	S	S	R	R	R	R
Klebsiella pneumoniae	H65	S	S	S	R	R	R	R
Klebsiella pneumoniae	H66	S	S	S	R	R	R	S
Klebsiella pneumoniae	H67	S	S	S	R	R	R	R
Klebsiella pneumoniae	H68	S	S	S	R	R	R	S
Klebsiella pneumoniae	H71	S	S	S	S	R	S	S

Table 4.1 (continue):

Klebsiella pneumoniae	H73	S	S	S	S	R	S	S
Escherichia coli	H8	S	S	S	R	R	R	R
Escherichia coli	H9	R	R	S	R	S	S	R
Escherichia coli	K16	S	S	S	R	R	R	R
Klebsiella pneumoniae	K21	R	S	R	R	R	R	R
Escherichia coli	K3	S	S	S	R	R	R	R
Klebsiella pneumoniae	P1	S	S	S	R	R	R	S
Escherichia coli	P4	S	S	S	S	R	R	R
Escherichia coli	P8	S	S	S	S	S	S	S
Pseudomonas aeruginosa	A6	S	S	S	S	R	R	S
Pseudomonas aeruginosa	K18	S	S	S	R	S	R	S
Pseudomonas aeruginosa	K2	S	S	S	S	R	R	S
Pseudomonas aeruginosa	K25	S	S	S	S	R	R	S
Pseudomonas aeruginosa	K5	S	S	S	R	S	R	S

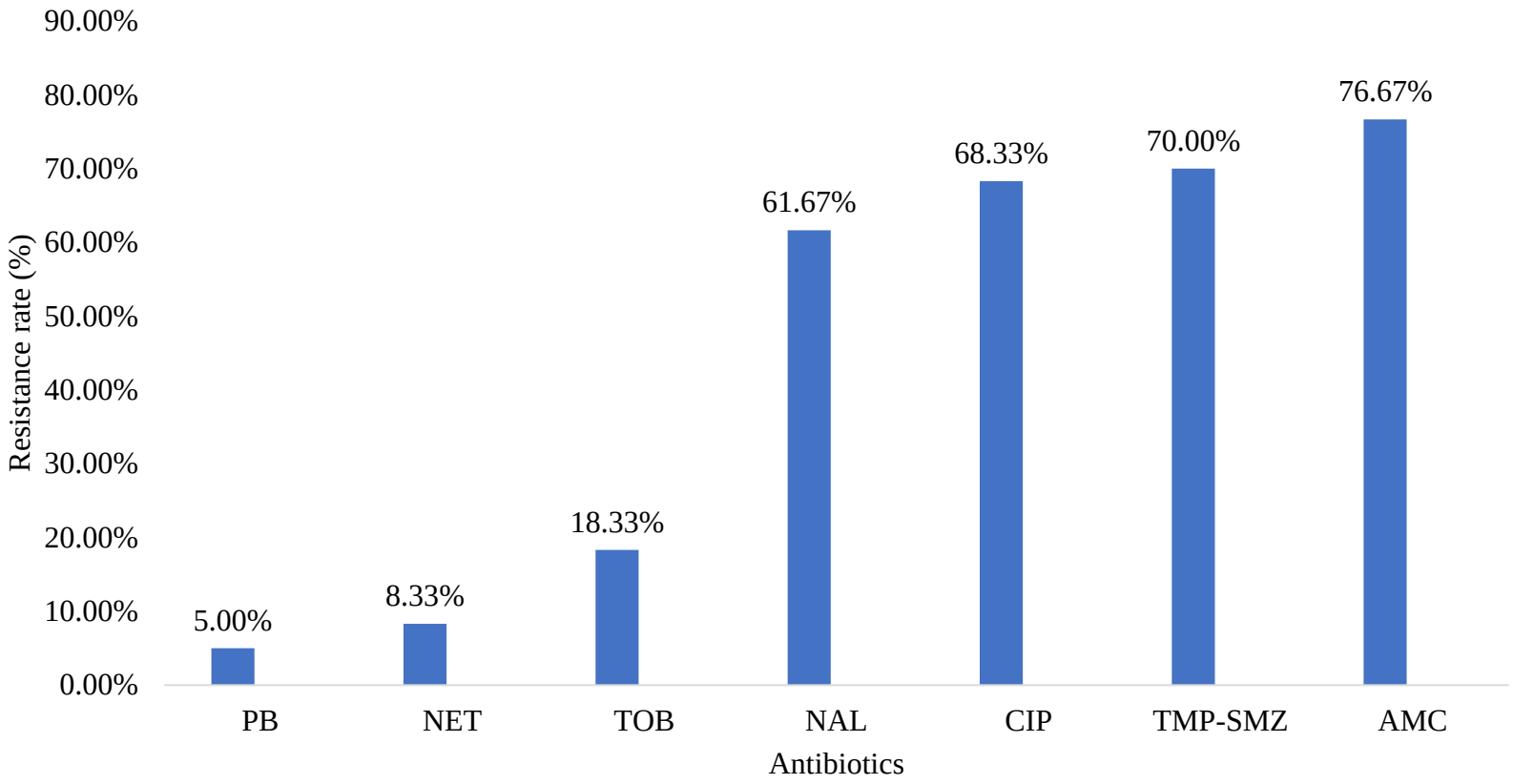

Figure 4.3: Antimicrobial resistance distribution patterns among clinical isolates (n = 60).

PB, Polymyxin B; NET, netillin; TOB, tobramycin; NAL, nalidixic acid; TMP-SMZ, trimethoprim-sulfamethoxazole; CIP, ciprofloxacin; AMC, amoxicillin-clavulanic acid.

4.4 Optimisation of Duplex PCR

After the screening of isolates for a few rounds by triplex PCR, only two *dfrA* genes (*dfrA1* and *dfrA7*) were identified. The annealing temperatures for detecting the *dfrA1* and *dfrA7* genes were optimised using two specific primer pairs. Figure 4.5 shows that the annealing temperatures ranged from 53.9℃ to 70.0℃. Based on the observation of the gel image, the most optimised annealing temperature for detecting the *dfrA1* and *dfrA7* genes is 63.6℃. Primer dimer was identified in the lane with annealing temperature of 66.8℃, so this temperature was excluded. The lanes with temperatures ranging from 63.6℃ to 53.9℃ exhibit promising bands with good intensity. However, the lane with PCR product at an annealing temperature of 60.0℃ showed the lowest intensity among these temperatures.

Although the annealing temperature was optimised, it was kept at 60.0℃ during the PCR runs as the final screening revealed the absence of *dfrA17* among the 60 isolates. According to Grape, et al. (2007), the annealing temperature for standard multiplex PCR for detection of *dfrA* genes is 60.0℃ when considering all three genes (*dfrA1*, *dfrA7*, and *dfrA17*) screened. To prevent non-specific primer binding to the DNA template and undesired amplification products, annealing temperatures below 60.0℃ were excluded. Therefore, the optimised annealing temperature could indicate necessary future amendments once positive isolates for *dfrA17* are obtained.

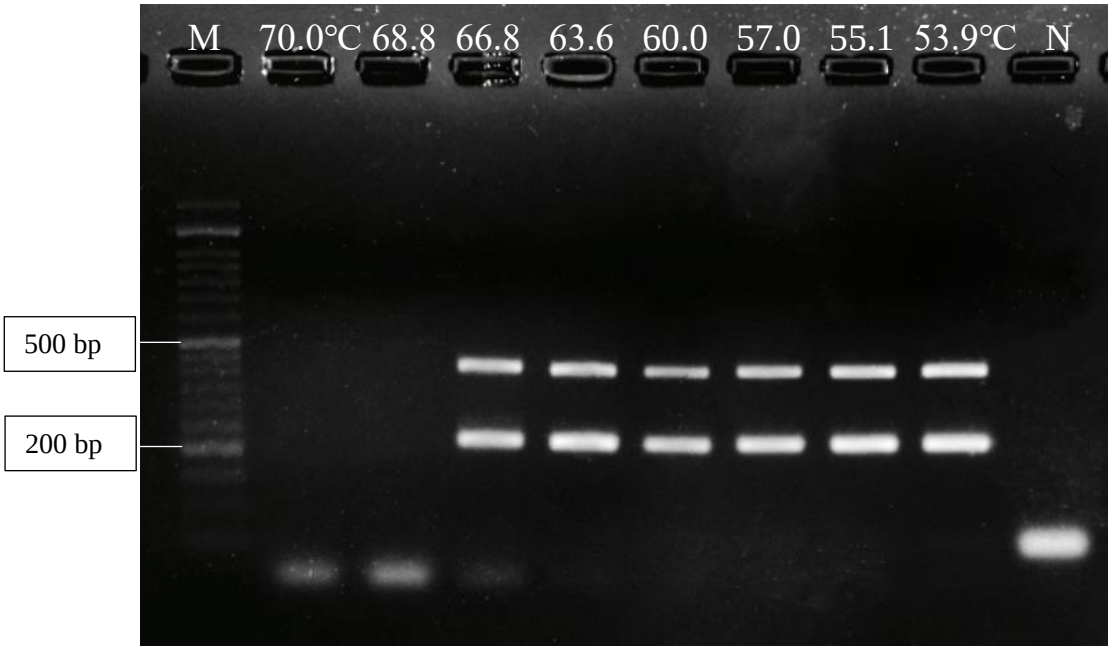

Figure 4.4: Gel image for Gradient PCR to optimise annealing temperature.

Gradient PCR was used to optimise the annealing temperature for both the *dfrA1* and *dfrA7* genes found in the bacterial isolates. Lane M represents the 50 bp DNA ladder. The numbers represent the annealing temperature in °C, while lane N indicates the lane loaded with negative control. Instead of DNA samples, distilled water was added as a negative control. The expected amplicon sizes for the *dfrA1* and *dfrA7* genes are 425 and 227 bp, respectively.

4.5 Concentration and Purity of DNA Extracted

The Nanodrop spectrophotometer was used to measure the purity (A260/A280 ratio) and concentration (ng/µl) of the isolated DNA. Data on DNA purity and concentration are given in Appendix C. Most DNA samples have a purity range of 1.8 to 2.0, which is considered to be pure DNA. However, several DNA samples fell outside this purity range due to RNA ($\geqslant$2.0) or protein ($\leqslant$1.6) contamination. This is because the DNA samples were extracted using the fast boil method, which allowed the isolated DNA to mix with the RNA and protein molecules found in the components of bacterial cells. The total DNA of these samples was extracted again until it reached a purity of 1.8 to 2.0.

4.6 Simultaneous Detection of Trimethoprim Resistance-Conferring (*dfrA*) genes among Bacterial Isolates

A total of 60 clinical bacterial isolates were screened by triplex PCR for the presence of the *dfrA1, dfrA7* and *dfrA17* genes. Figure 4.6 shows the PCR amplification of the *dfrA* genes with expected amplicon sizes of 425 bp (*dfrA1*), 227 bp (*dfrA7*) and 171 bp (*dfrA17*). Eight (13.33%) of the 60 bacterial isolates tested positive for *dfrA1*, nine (15.00%) for *dfrA7* and none had the *dfrA17* gene (Figure 4.7). Clinical bacterial isolates had a higher frequency of the *dfrA7* gene than the *dfrA1* and *dfrA17* genes. None of the bacterial strains examined in this study had all three *dfrA* genes coexisting in one. In addition, no *P. aeruginosa* strain was tested positive for any of the *dfrA* genes.

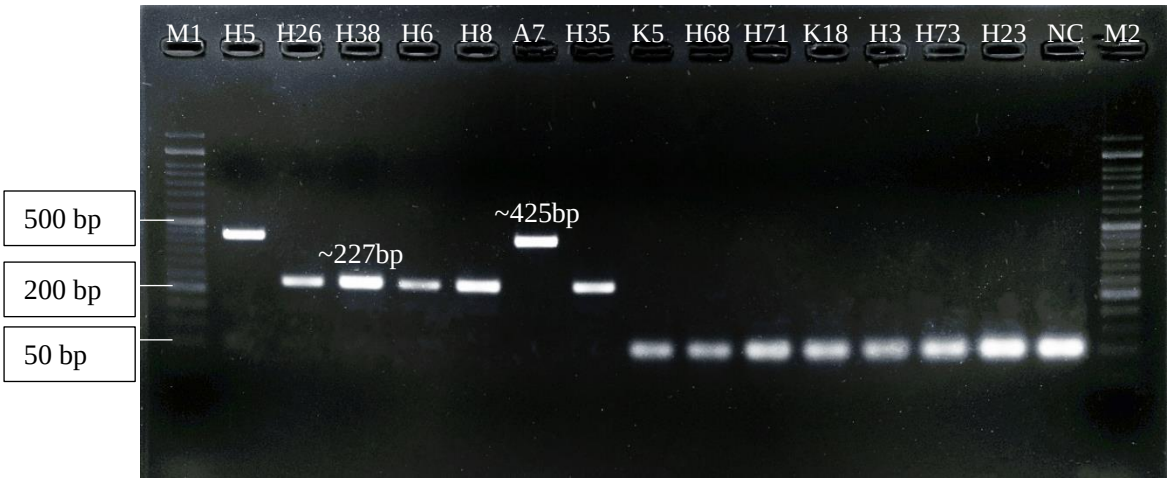

Figure 5: Representative gel image of a triplex polymerase chain reaction for the simultaneous detection of the *dfrA1, dfrA7* and *dfrA17* genes.

Lanes M1 and M2 were loaded with the 50 bp DNA ladder to act as a molecular weight marker. The remaining lanes were loaded with DNA samples isolated from the bacterial strains as indicated in the gel image. Lane NC represents the negative control where sterile distilled water was used instead of the DNA samples. The expected amplicon sizes for *dfrA1, dfrA7* and *dfrA17* are 425 bp, 227 bp and 171 bp respectively. From the gel image provided, the H5 and A7 strains tested positive for *dfrA1*, while the other strains (H26, H38, H6, H8 and H35) tested positive for *dfrA7* genes. The remaining lanes did not show the expected amplification products, indicating that the isolates were negative for the *dfrA* genes. Due to the non-optimised conditions of the PCR, the presence of a primer dimer was observed at 50 bp.

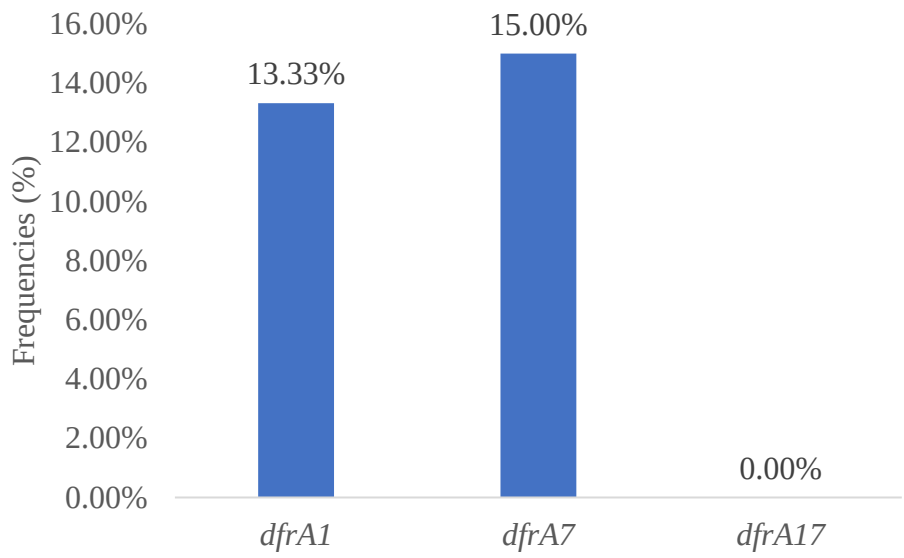

Figure 4.6: Distribution (%) of the *dfrA* gene in the clinical isolates.

4.7 Distribution of *dfrA* genes across Different Gender and Age Groups

The distribution of the two *dfrA* genes (*dfrA1* and *dfrA7*) was tabulated according to age groups and gender, and statistical analysis of the association between the presence of *dfrA* genes and these demographic parameters, such as gender and age group, was performed. Appendix D provides representative data for statistical analysis on the association between *dfrA* genes and demographic profiles. The *dfrA17* gene was not included in the analysis due to its absence in the clinical isolates tested.

Regarding gender, the prevalence of *dfrA1* is slightly higher in males (13.89%) than in females (12.50%), as shown in Figure 4.8. On the other hand, the prevalence of the *dfrA7* gene is approximately twice as high in males (19.44%) compared to females (8.33%). Male patients showed a comparably higher prevalence of total positive isolates for the *dfrA* genes than female patients.

However, there is no positive association ($p > 0.05$) between the gender of the patients and the distribution of *dfrA* genes, as shown in the statistical analysis in Table 4.2. In terms of age groups (Figure 4.9), the working age group contains the highest prevalence of *dfrA*-positive isolates. The prevalence of the *dfrA1* gene was higher than that of the *dfrA7* gene in both the young and working age groups, with percentages of 16.67% and 21.74%, respectively. However, the *dfrA1* gene has a lower prevalence in the old age group (6.45%) compared to *dfrA7*. The *dfrA7* gene is the most common gene (19.35%) in the old age group compared to the working age group (13.04%) and is absent in the young age group (0.00%). Nevertheless, the prevalence of the *dfrA1* and *dfrA7* genes is not positively associated with the different age groups of patients.

Table 4.2: Distribution of *dfrA1* and *dfrA7* genes by gender and age group.

Demographic details		**Multiplex PCR *dfrA* genes detection**					
		dfrA1+	***dfrA1-***	***p*-value**	***dfrA7+***	***dfrA7-***	***p*-value**
Gender	**Female (n=24)**	3 (12.50%)	21 (87.50%)	0.877	2 (8.33%)	22 (91.67%)	0.293
	Male (n=36)	5 (13.89%)	31 (86.11%)		7 (19.44%)	29 (80.56%)	
Age group	**Young age (n=6)**	1 (16.67%)	5 (83.33%)	0.255	0 (0.00%)	6 (100.00 %)	0.452
	Working age (n=23)	5 (21.74%)	18 (78.26%)		3 (13.04%)	20 (86.96%)	
	Old age (n=31)	2 (6.45%)	29 (93.55%)		6 (19.35%)	25 (80.65%)	

*A *p*-value of less than 0.05 is considered to be statistically significant.

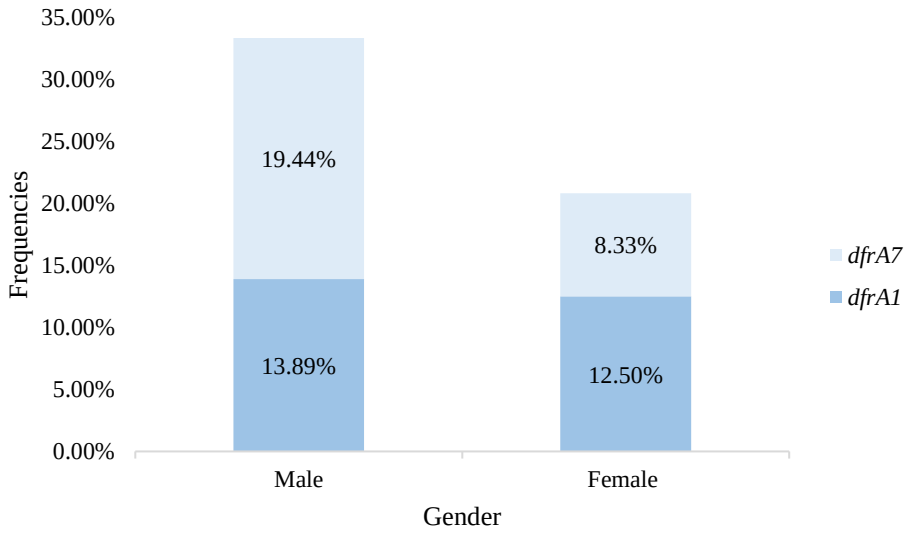

Figure 4.7: Distribution of *dfrA* genes according to patient gender.

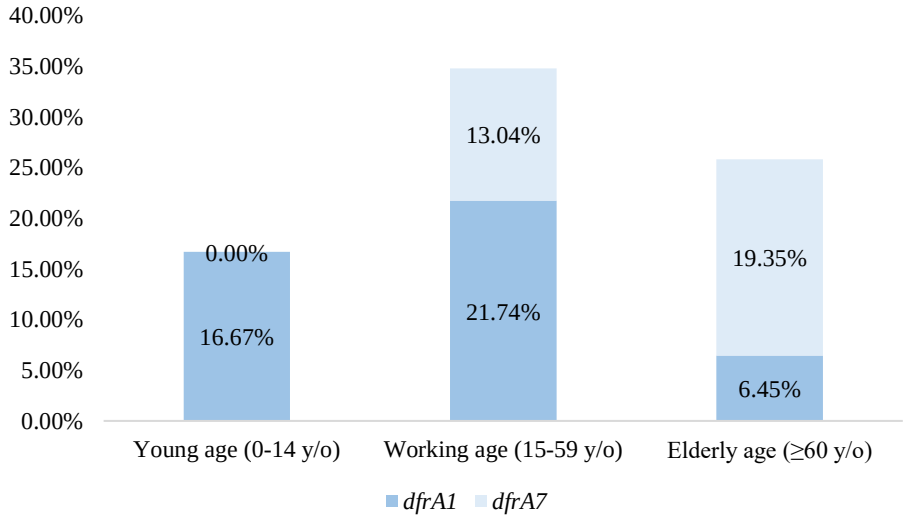

Figure 4.8: Distribution of *dfrA* genes according to patient age groups.

4.8 Correlation between the Antimicrobial Resistance Phenotypic Traits and the Genotypic Profile of Clinical Isolates

According to Table 4.3, the association between the genotypic profile and the phenotypic profile of the antimicrobial resistance of the clinical isolates was identified by performing the *Chi*-square analysis or Fisher's exact test.

Appendix E provides representative data for statistical analysis on the association between *dfrA* genes and phenotypic profiles. Of the total 60 clinical isolates, 42 (70.00%) were resistant to trimethoprim-sulfamethoxazole. Among the trimethoprim-sulfamethoxazole resistant isolates, the number of isolates found to carry the *dfrA1* gene and the *dfrA7* gene is eight (19.04%) and nine (21.43%), respectively (Figure 4.10). None of the susceptible isolates carried the antibiotic resistance gene. The moderately high distribution of *dfrA* genes in the trimethoprim-sulfamethoxazole resistant isolates may indicate a possible positive association between the genotypic profile and the phenotypic profile of antimicrobial resistance. After further identification using statistical analysis, it was found that the distribution of the *dfrA7* gene within the isolates was positively associated with the trimethoprim-sulfamethoxazole antimicrobial resistance phenotypes, with the *p*-value obtained being 0.047. Nevertheless, the *dfrA1* gene was found to be negatively associated with the phenotypic profile of antimicrobial resistance towards trimethoprim-sulfamethoxazole.

Otherwise, the distribution of *dfrA7* genes was found to positively correlate with the antimicrobial resistance phenotypes of other classes of fluoroquinolone antibiotics such as ciprofloxacin, where the *p*-value obtained is 0.027. However, a negative association of the *dfrA1* gene with the ciprofloxacin antibiotic resistance phenotypic profile was observed ($p = 0.211$). Meanwhile, the distribution of *dfrA* genes was negatively associated ($p > 0.05$) with the rest of the antimicrobials tested, namely netillin, amoxicillin-clavulanic acid, polymyxin B, nalidixic acid and tobramycin (Table 4.4).

Figure 4.9: Distribution of *dfrA1* and *dfrA7* genes based on trimethoprim-sulfamethoxazole phenotypic resistance profiles of isolates.

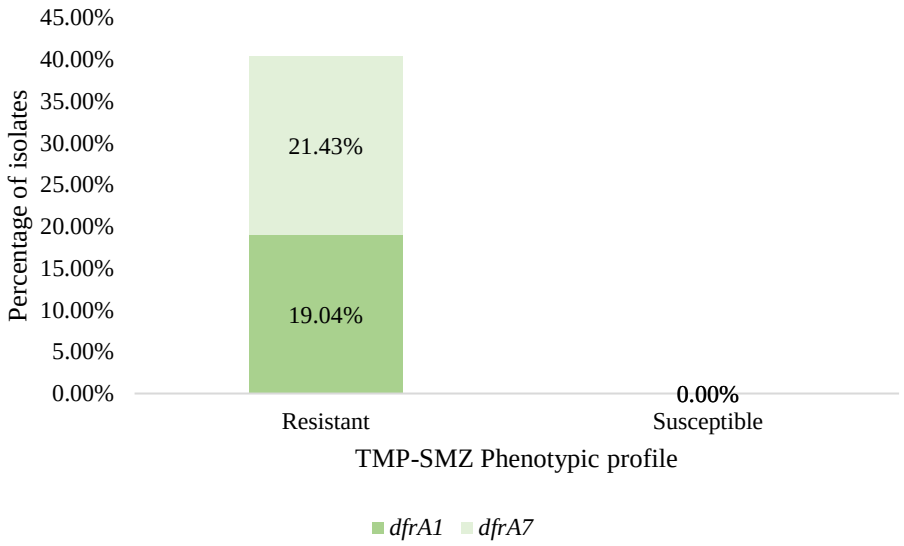

Table 4.3: Results of genotypic profile of clinical isolates from PCR assay and their phenotypic resistance profile to trimethoprim-sulfamethoxazole.

Species	Sample	TMP-SMZ	*dfrA1*	*dfrA7*	*dfrA17*
Escherichia coli	A7	R	+	-	-
Enterobacter cloacae	G21	S	-	-	-
Morganella morganii	G52	S	-	-	-
Citrobacter freundii	G63	R	-	-	-
Enterobacter aerogenes	G66	S	-	-	-
Enterobacter cloacae	G69	R	+	-	-
Escherichia coli	G7	R	-	-	-
Escherichia coli	H12	R	+	-	-
Klebsiella pneumoniae	H14	S	-	-	-
Klebsiella pneumoniae	H15	R	-	-	-
Klebsiella pneumoniae	H16	S	-	-	-
Klebsiella pneumoniae	H19	S	-	-	-
Escherichia coli	H21	R	-	-	-
Klebsiella pneumoniae	H22	S	-	-	-
Enterobacter amnigenus	H23	S	-	-	-
Klebsiella pneumoniae	H26	R	-	+	-
Klebsiella pneumoniae	H27	S	-	-	-
Klebsiella pneumoniae	H28	R	-	-	-
Escherichia coli	H3	S	-	-	-
Klebsiella pneumoniae	H31	R	-	-	-
Klebsiella pneumoniae	H32	R	-	+	-
Escherichia coli	H33	R	-	-	-

Table 4.3 (continue):

Klebsiella pneumoniae	H34	S	-	-	-
Escherichia coli	H35	R	-	+	-
Klebsiella pneumoniae	H38	R	-	+	-
Klebsiella pneumoniae	H4	S	-	-	-
Klebsiella pneumoniae	H40	R	-	-	-
Escherichia coli	H41	R	-	-	-
Klebsiella pneumoniae	H43	R	-	-	-
Klebsiella pneumoniae	H45	R	-	-	-
Enterobacter cloacae	H5	R	+	-	-
Escherichia coli	H52	R	-	+	-
Escherichia coli	H54	R	+	-	-
Klebsiella pneumoniae	H55	R	-	-	-
Klebsiella pneumoniae	H56	S	-	-	-
Klebsiella pneumoniae	H57	S	-	-	-
Klebsiella pneumoniae	H58	R	-	-	-
Escherichia coli	H59	R	-	+	-
Klebsiella pneumoniae	H6	R	-	+	-
Klebsiella pneumoniae	H62	R	-	-	-
Klebsiella pneumoniae	H63	R	-	-	-
Klebsiella pneumoniae	H65	R	-	-	-
Klebsiella pneumonia	H66	R	-	-	-
Klebsiella pneumoniae	H67	R	+	-	-
Klebsiella pneumoniae	H68	R	-	-	-
Klebsiella pneumoniae	H71	S	-	-	-
Klebsiella pneumoniae	H73	S	-	-	-
Escherichia coli	H8	R	-	+	-
Escherichia coli	H9	S	-	-	-
Escherichia coli	K16	R	-	-	-
Klebsiella pneumoniae	K21	I	-	-	-
Escherichia coli	K3	R	+	-	-
klebsiella pneumoniae	P1	R	-	+	-
Escherichia coli	P4	R	+	-	-
Escherichia coli	P8	S	-	-	-
Pseudomonas aeruginosa	K2	R	-	-	-
Pseudomonas aeruginosa	K5	R	-	-	-
Pseudomonas aeruginosa	K25	R	-	-	-
Pseudomonas aeruginosa	A6	R	-	-	-
Pseudomonas aeruginosa	K18	R	-	-	-

Table 4.4: Association between *dfrA* genes and the antimicrobial resistance profile of the clinical isolates.

Antimicrobial susceptibility		Multiplex PCR *dfrA* genes detection					
		***dfrA1* +**	***dfrA1* -**	***p*-value**	***dfrA7* +**	***dfrA7* -**	***p*-value**
Netillin*	R (n=5)	0 (0.0%)	5 (100.0%)	1.000	4 (80.0%%)	1 (20.0%)	0.570
	S (n=55)	8 (14.5%)	47 (85.5%)		8 (14.5%)	47 (85.5%)	
TMP-SMZ*	R (n=42)	8 (19.0%)	34 (81.0%)	0.091	9 (21.4%)	33 (78.6%)	**0.047**
	S (n=18)	0 (0.0%)	18 (100.0%)		0 (0.0%)	18 (100.0%)	
AMC*	R (n=46)	8 (17.4%)	38 (82.6%)	0.179	9 (19.6%)	37 (80.4%)	0.100
	S (n=14)	0 (0.0%)	14 (100.0%)		0 (0.0%)	14 (100.0%)	
Polymyxin B*	R (n=3)	0 (0.0%)	3 (100.0%)	1.000	0 (0.0%)	3 (100.0%)	1.000
	S (n=57)	8 (14.0%)	49 (86.0%)		9 (15.8%)	48 (84.2%)	
Ciprofloxacin*	R (n=41)	7 (17.1%)	34 (82.9%)	0.416	9 (22.0%)	32 (78.0%)	**0.046**
	S (n=19)	1 (5.3%)	18 (94.7%)		0 (0.0%)	19 (100.0%)	
Nalidixic acid*	R (n=37)	7 (18.9%)	30 (81.1%)	0.138	7 (18.9%)	30 (81.1%)	0.460
	S (n=23)	1 (4.3%)	22 (95.7%)		2 (8.7%)	21 (91.3%)	
Tobramycin*	R (n=11)	1 (9.1%)	10 (90.9%)	1.000	1 (9.1%)	10 (90.9%)	1.000
	S (n=49)	7 (14.3%)	42 (85.7%)		8 (16.3%)	41 (83.7%)	

'**R**' indicates resistant isolates; '**S**' indicates susceptible isolates.

**P* value for the analysis of the antimicrobial susceptibility profile in *dfrA*-positive and *dfrA*-negative isolates was determined using Pearson's χ^2 test. Bolded *P* values less than 0.05 are considered statistically significant.

*Fisher's exact test was used when at least one cell (20%) of the contingency table had an expected cell count of <5.

CHAPTER 5

DISCUSSION

5.1 Overview

In this study, the distribution of the *dfrA* genes was determined using triplex PCR, and the antimicrobial susceptibility of the clinical isolates was tested against seven types of antibiotics to identify the antimicrobial phenotypic resistance profiles of the isolates. Furthermore, the association between the genotypic profile and the phenotypic resistance profile of the isolates, as well as the patient's age and gender, were evaluated using the *Chi*-square test or Fisher's exact test.

5.2 Antimicrobial Susceptibility Patterns of Clinical Isolates

Figure 4.3 shows that clinical isolates are the most resistant to amoxicillin-clavulanic acid (76.67%). The increased rate of resistance could be attributed to the widespread use of amoxicillin-clavulanic acid in the treatment of bacterial infections. The previous use of AMC for therapy may have led to the development of resistance (Oteo, et al., 2008). The AMC was first presented for clinical usage in 1984 and has been in use for decades. Because of the widespread use of antibiotics to treat bacterial infections, many clinical isolates have developed antibiotic resistance due to selective pressure (National Institute of Diabetes and Digestive and Kidney Diseases, 2020). Amoxicillin-clavulanic acid resistance is mostly caused by TEM-1 β-lactamase overproduction in *E. coli* or co-expression either with OXA-2-like and/or SHV β-lactamases in *K. pneumoniae* (Di Conza, et al., 2014).

The antimicrobial susceptibility test demonstrated that the clinical isolates were very resistant (70.00%) to trimethoprim-sulfamethoxazole, which is comparably similar to studies conducted in Iran (69.80%) and the United States of America (71.00%) (Yadav, et al., 2015; Luterbach, et al., 2018). The current study found a higher resistance rate to TMP-SMZ compared to the findings by Marchant, et al. (2013) whereby the *E. coli* collected from swine faecal samples showed 67.5% of trimethoprim-sulfamethoxazole resistance. The study also shows higher rates of trimethoprim-sulfamethoxazole resistance compared to a study conducted in Nepal among the *Enterobacteriaceae* isolates (62.11%) (Yekani, et al., 2018). Trimethoprim-sulfamethoxazole is commonly used as a first-line empiric therapeutic medication for the treatment of acute uncomplicated cystitis and the long-term prevention and treatment of urinary tract and respiratory infections. Nevertheless, its widespread clinical use has led to an increase in resistance, mainly due to the horizontal transmission of class 1 integrons in *Enterobacteriaceae*. Class 1 integron is usually linked to other antibiotic resistance genes, such as *sul1*, which provides resistance to sulfamethoxazole (van der Veen, et al., 2009).

The study found high rates of resistance to quinolone and fluoroquinolone antibiotics, particularly nalidixic acid (61.67%) and ciprofloxacin (68.33%). In Nepal, resistance to nalidixic acid was even higher at 81.05%, while an investigation in Iran reported a slightly lower rate of 68.90% (Yadav, et al., 2015; Yekani, et al., 2018). In this study, it was found that 68.33% of clinical isolates were resistant to ciprofloxacin. This rate is higher than the rates reported in Nepal (61.05%) and Iran (66.20%) (Yadav, et al., 2015; Yekani, et al., 2018).

Ciprofloxacin is a newer generation of quinolones compared to nalidixic acid, with a wider range of antibacterial activities. The increased rate of resistance to ciprofloxacin may be due to its broader spectrum of bacterial species targeted, which increases the evolutionary selective pressure on bacterial populations (Martijn Sijbom, et al., 2023). The resistance of bacteria to fluoroquinolones may be linked to the increased use of antibiotics to treat infections. Bacterial resistance has gradually increased since an earlier study showed that *E. coli* was completely sensitive to fluoroquinolones. Excessive antibiotic pressure can induce a high rate of antibiotic resistance via the chromosomally encoded fluoroquinolone resistance gene and plasmid-mediated quinolone resistance (PMQR) genes (Jafri, et al., 2014).

The clinical isolates in this study exhibit a low resistance rate to polymyxin B. This low level of resistance may be due to reduced use in clinical settings, as the drug can cause significant side effects such as nephrotoxicity and neurotoxicity, particularly when administered parenterally (Poirel, Jayol and Nordmann, 2017; da Silva, 2022). Only 3 out of the 55 isolates (5.00%) were found to be resistant to polymyxin B. The resistance rates for aminoglycoside antibiotics, such as netillin (8.33%) and tobramycin (18.33%), were also determined. The resistance to tobramycin is considered high compared to similar studies conducted in Switzerland (9.30%), France (7.70%), Germany (6.90%), and Austria (6.90%) (Bodendoerfer, et al., 2020). Tobramycin is frequently used in combination with beta-lactam antibiotics to enhance its antibacterial activity. The widespread use of tobramycin in the treatment of bacterial infections may also have contributed to the development of resistance.

Antibiotic resistance can be caused or spread by various circumstances, including unreasonable antibiotic use. Additionally, antimicrobial susceptibility rates vary over time. Therefore, continuous surveillance of antimicrobial resistance is necessary to maintain the safety of empirical antibiotic therapy and prevent the spread of antimicrobial resistance (Jafri, et al., 2014).

5.3 Prevalence of *dfrA* genes within the Bacterial Isolates

The study reveals that the incidence of *dfrA7* genes (15.00%) is higher than that of *dfrA1* genes (13.33%), but *dfrA17* genes (0.00%) are absent in all isolates analysed. These findings contrast with those of a study of uropathogenic *Escherichia coli* (UPEC) isolates from Canada and Europe, which found that *dfrA1* had the highest frequency (40.00%), followed by *dfrA17* (31.11%), and the least prevalent gene was *dfrA7* (4.44%) (Blahna, et al., 2006). Furthermore, a study carried out in Australia found that *dfrA17* was more common than *dfrA1* in *Enterobacteriaceae* isolates, which contrasts with the results of this study (White, McIver and Rawlinson, 2001). In addition, *dfrA12* was the most common gene found in the isolates along with *dfrA17* (White, McIver and Rawlinson, 2001). The studies conducted in Turkey, Korea and Syria have reported similar results, with the prevalence of *dfrA7* and *dfrA17* being higher than that of *dfrA1* among isolates (Sandalli, et al., 2009; Yu, 2004; Al-Assil, Mahfoud and Hamzeh, 2013).

In a Malaysian study (Kor, Choo, and Chew, 2013), the amplified gene cassettes of multidrug-resistant *Enterobacteriaceae* and *Pseudomonas aeruginosa* strains revealed the prevalence of *dfrA1* (28.57%), *dfrA7* (9.52%) and *dfrA17* (2.38%).

When compared to this study, these results show similar trends with the prevalence of *dfrA17* genes (2.38%) being the lowest compared to other *dfrA* genes. However, *dfrA12* (11.90%) was found to be more prevalent than *dfrA7* and *dfrA17* but less prevalent than *dfrA1* (28.57%), suggesting the need for future research into the frequency of the *dfrA12* gene in clinical isolates in relation to trimethoprim-sulfamethoxazole resistance.

These findings indicate that the incidence of *dfrA* genes varies geographically. In a study of *E. coli* in Lithuania, the prevalence of *dfrA17* (8.20%) was higher than that of *dfrA1* (7.40%) (Šeputienė, et al., 2010). The distribution of *dfr* genes may differ because they originated in diverse regions and then expanded to geographically distant areas (Lee, et al., 2001). Therefore, the findings of this study do not agree with Grape, et al. (2007), who reported that *dfrA17* was one of the most prevalent *dfr* genes, in addition to *dfrA1*, *dfrA5*, *dfrA7*, and *dfrA12*, within bacterial isolates.

The incidence of *dfrA* genes varied among different bacterial isolates, as reported by Brolund, et al. (2010). The highest prevalence of *dfrA1* was found in *E. coli* and *K. pneumoniae*, followed by *dfrA17*, which was also prevalent in *E. coli* but only found in one *K. pneumoniae* isolate (Brolund, et al., 2010). Therefore, this data may indicate variations in the frequency of *dfrA* genes among bacterial species, aside from their distinct distribution in different geographical regions.

5.4 Association between Phenotypic Profile and *dfrA* gene Profile

The study discovered a positive correlation ($p < 0.05$) between the presence of the *dfrA7* genes and antimicrobial resistance to trimethoprim-sulfamethoxazole among the bacterial isolates. Additionally, the fluoroquinolone class of antibiotics, which includes ciprofloxacin, is significantly correlated with the existence of *dfrA7*. However, there is no positive correlation between the *dfrA1* gene and ciprofloxacin and trimethoprim-sulfamethoxazole antibiotic resistance. The *dfr* genes encode the dihydrofolate reductase enzyme, which is resistant to trimethoprim due to an altered active site (Kester, Karpa and Vrana, 2012). It is important to consider both the *dfr* and *sul* genes simultaneously as they are involved in conferring resistance to trimethoprim-sulfamethoxazole. The *sul* genes encode for a mutant enzyme with no binding affinity to the sulfonamides. In the study by Amador, et al. (2019), it was found that trimethoprim-sulfamethoxazole resistant isolates harboured at least one type of gene from either *dfr* or *sul* genes. The mutant enzyme hinders the sequential inhibition of the enzyme involved in the folate pathway by trimethoprim-sulfamethoxazole, reducing its bactericidal effects and leading to higher resistance rates in bacterial isolates.

The *dfrA* gene, responsible for trimethoprim resistance, is frequently linked to class 1 or 2 integrons that can contain various types of exogenous gene cassettes. The acquisition of mobile genetic elements (MGEs) that provide antibiotic resistance can hasten the dissemination of multidrug resistance among bacterial isolates. Figure 2.7 shows that the integron comprises a variable region flanked by the 5' and 3' conserved regions. The variable region may contain various

types of antibiotic resistance genes, such as the *dfrA1* gene. Additionally, the *sul* gene, which is integrated into the 3' conserved region of the integron, contributes to resistance against sulfonamides. Therefore, it is possible that the bacterial isolates examined in this study contain *dfr* and *sul* resistance genes linked to an integron. However, the influence of integrons in the transmission of *dfr* and *sul* genes among bacterial isolates, which are positively associated with trimethoprim-sulfamethoxazole resistance (Rajpara, et al., 2015), was not investigated in this study. In Malaysia, Kor, Choo, and Chew (2013) found a high incidence of integron-positive *Enterobacteriaceae* and *P. aeruginosa* with *dfr* genes.

Further study is required to determine the association between the *sul* genes and trimethoprim-sulfamethoxazole resistance. Integrons carrying both the *sul* and *dfr* genes are frequently coexistent. The *dfr* and *sul* genes are often arranged sequentially within the same integron. The majority of *dfrA* genes were linked to either *ISCR2*, which is typically associated with the *sul2* gene, or *ISCR1*, which is downstream of *sul1* (Jiang, et al., 2023; Rajpara, et al., 2015). This study found that not all trimethoprim-sulfamethoxazole resistant isolates contain the targeted *dfrA* genes. Specifically, *dfrA1* was present in 19.00% of the TMP-SMZ resistant isolates and *dfrA7* was present in 21.43% of the TMP-SMZ resistant isolates. It is possible that the targeted *dfrA* genes are not the primary mechanism for conferring trimethoprim-sulfamethoxazole resistance. The bacterial isolates may carry one or more of the other 30 over different *dfr* genes that were not targeted in the PCR assay in this study, which could be associated with TMP-SMZ resistance (Somorin, et al., 2022).

Additionally, the phenotypic profile of ciprofloxacin resistance may be linked to the dissemination of antibiotic resistance genes. This involves mutations in the DNA gyrase and topoisomerase genes, namely *gyrA* and *parC*, respectively, as well as plasmid-mediated quinolone resistance (PMQR) genes, such as *qnrA*, *qnrB* and *qnrS* (Morgan-Linnell, et al., 2008; Pérez-Legaspi and Rico-Martínez, 2023). According to An (2023), fluoroquinolone resistance in UPEC bacterial isolates was most likely induced by a DNA mutation in the *gyr* or *par* genes, which encode the fluoroquinolone target enzyme. Aside from that, the *qnr* genes can be expressed on the plasmid alongside the integron-carried *dfrA* genes, providing resistance to both fluoroquinolones and trimethoprim-sulfamethoxazole (Abdel-Rhman, Elbargisy, and Rizk, 2021).

5.5 Association between the *dfrA* genes Prevalence and the Age/Gender Distribution of Patients

The statistical analysis did not reveal a significant association between the prevalence of *dfrA* genes and the demographic profiles of patients, including age and gender. Although there was no significant correlation between the *dfrA* genes and the age groups of the patients, the working age group of patients had a significantly higher prevalence of *dfrA1* positive isolates, while the old age group had a higher prevalence of *dfrA7*. According to the overall trend, *dfrA* positive isolates are more prevalent in the working age groups, followed by the old age group and finally the young age group.

The *dfrA1* gene has the highest frequency in the working age group, followed by the young age group. The *dfrA7* gene was found more frequently in the old age group, with the highest frequencies, followed by the working age group.

Wang, et al. (2023) found a negative association between the resistance rate and age group, indicating that the phenotypic profile is not correlated with the different age groups of patients. The higher prevalence of the *dfrA* gene among the working-age and old groups may be due to their increased exposure to multidrug-resistant (MDR) bacteria when visiting hospitals and medical centres. Patients may acquire healthcare-associated infections (HAI) from MDR strains. If hospitalised, patients may be exposed to the patient-to-patient transmission of MDR strains in areas with poor hygiene or environmental contamination.

Moreover, antimicrobial-resistant bacteria are prevalent in nursing homes, and residents may also be colonised by antimicrobial resistant bacteria (Rowan-Nash et al., 2020). It has been identified that the accumulation of antibiotic resistance genes becomes more complex as the age group increases, with a higher abundance of antimicrobial resistance genes found. Therefore, it is hypothesised that patients in the working age group and the old age group who are exposed to microbes more frequently are at a higher risk of developing antibiotic resistance (Wu, et al., 2021).

The study also revealed a higher proportion of *dfr*-positive clinical specimens from males, who are at higher risk of infection with AMR bacteria due to several factors, including differences in the underlying biological response, such as the immune response, variations in antibiotic prescribing and lower hand hygiene compliance among men (Brandl, et al., 2021).

5.6 Limitations and Future Study

Although this study found a significant level of resistance to most antibiotics tested, the sample size (n = 60) was insufficient when compared to previous studies that recruited a few thousand bacterial isolates. Due to time constraints and a restricted workforce, this study had a smaller sample size. More isolates from East Malaysia are necessary to make a definite observation on the frequency of the antibiotic resistance phenotypic profile in clinical samples within a larger epidemiological aspect of Malaysia. As a result, a larger sample size is necessary to determine the prevalence of antibiotic resistance in various Malaysian hospitals. In addition, because the bacterial isolates were collected before the COVID-19 era, the prevalence of AMR among clinical isolates may not fully reflect the current level of resistance among bacterial isolates. Future studies can include the currently available isolates, as the COVID-19 pandemic may have increased the prevalence of AMR and the growth of resistant isolates by diverting healthcare resources away from AMR surveillance and management.

Furthermore, the existence of integrons and integron-carrying genes, such as the *sul* genes, was not explored in this study to determine their implications on phenotypic resistance to trimethoprim-sulfamethoxazole. A future study should include these genes to have a better understanding of the antibiotic resistance genes that confer resistance to trimethoprim-sulfamethoxazole. Aside from that, other *dfr* gene variations with high prevalence observed in previous studies, such as *dfrA12*, should be studied to determine their prevalence among multidrug-resistant clinical isolates.

The study lacked sufficient samples from each bacterial species to conduct a *Chi*-square test or Fisher's exact test and establish a significant correlation between the antibiotic resistance gene included in this study and each type of bacterial isolate. For example, there is only one strain for some of the bacterial species revived, which are *Morganella morganii*, *Enterobacter amnigenus*, *Enterobacter aerogenes*, and *Citrobacter freundii*. Additionally, our study's triplex PCR runs did not have a positive control for *dfrA17* to confirm the accuracy of the PCR assay for the target gene amplification. Thus, the absence of *dfrA17* in this study could be attributed to false negative results, as there was no positive control. Furthermore, DNA sequencing needs to be done in future studies to verify the identity of the amplicons generated. The sequence should then be compared to databases using the NCBI BLAST tool to ensure the correct sequence of the amplified PCR products was obtained in the PCR assays by using the specific primer pairs.

CHAPTER 6

CONCLUSION

The objective of this study was to screen for the *dfrA* genes (*dfrA1*, *dfrA7* and *dfrA17*) conferring resistance to trimethoprim-sulfamethoxazole by performing triplex PCR among the multidrug-resistant bacterial isolates collected from different hospitals distributed in West Malaysia. The Kirby-Bauer disc diffusion method was used in this study to determine the susceptibility of the 60 clinical bacterial isolates to different types of antibiotics such as amoxicillin-clavulanic acid, trimethoprim-sulfamethoxazole, nalidixic acid, ciprofloxacin, netillin, tobramycin and polymyxin B.

Subsequently, the association between the presence of *dfrA* genes and the antibiotic resistance profile as well as the age and gender of the patient was determined by using the *Chi*-square test or Fisher's exact test. In this study, eight (13.33%) and nine (15.00%) of the 60 bacterial isolates were screened positive for *dfrA1* and *dfrA7*, respectively. None of the isolates were screened positive for the *dfrA17* genes. Overall, the presence of both *dfrA1* and *dfrA7* genes outnumbered the *dfrA17* genes among clinical bacterial isolates. The clinical isolates had the highest resistance rate to amoxicillin-clavulanic acid (76.67%), followed by trimethoprim-sulfamethoxazole (70.00%), ciprofloxacin (68.33%), nalidixic acid (61.67%), tobramycin (18.33%), netillin (8.33%), and lastly polymyxin B (5.00%).

Statistical analysis revealed a significant association between the *dfrA7* genes

and antibiotic resistance phenotypes against ciprofloxacin and trimethoprim-sulfamethoxazole, whereas the *dfrA1* gene was not associated with any antimicrobial resistance phenotypes with a *Chi*-square value greater than 0.05. Otherwise, patients' age and gender also showed a negative association with the presence of the *dfrA* genes.

This study successfully shows the distribution and prevalence of *dfrA* genes among clinical isolates, with *dfrA7* conferring resistance to ciprofloxacin and trimethoprim-sulfamethoxazole. This could possibly be related to the presence of the plasmid containing the PMQR and gene cassettes containing the *dfrA* genes that confer the multidrug resistance profile in the bacterial isolates. However, the high rate of trimethoprim-sulfamethoxazole resistance among clinical isolates suggests that antibiotic therapy with trimethoprim-sulfamethoxazole should be closely regulated before prescribing it to the patient, with antimicrobial susceptibility testing performed to avoid ineffective therapy. To maintain the efficacy of present broad-spectrum antibiotics, antibiotic therapy must be tightly managed to prevent the formation of more extensively antibiotic-resistant isolates as a result of the selective pressure induced by improper antibiotic prescription.

REFERENCES

Abdel-Rhman, S. H., Elbargisy, R. M., and Rizk, D. E., 2021. Characterization of integrons and quinolone resistance in clinical *Escherichia coli* isolates in Mansoura City, Egypt. *International Journal of Microbiology*, 2021, pp.1–11.

Al-Ajmi, D., Rahman, S. and Banu, S., 2020. Occurrence, virulence genes, and antimicrobial profiles of *Escherichia coli* O157 isolated from ruminants slaughtered in Al Ain, United Arab Emirates. *BMC Microbiology*, 20(1), pp.1–10.

Alajmi, R.Z., Alfouzan, W.A., and Mustafa, A.S., 2023. The prevalence of multidrug-resistant *Enterobacteriaceae* among neonates in Kuwait. *Diagnostics*, 13(8), pp.1505–1505.

Al-Assil, B., Mahfoud, M. and Hamzeh, A.R., 2013. First report on class 1 integrons and Trimethoprim-resistance genes from *dfrA* group in uropathogenic *E. Coli* (UPEC) from the Aleppo area in Syria. *Mobile Genetic Elements*, 3(3), pp.1–6.

Alkofide, H., Alhammad, A.M., Alruwaili, A., Aldemerdash, A., Almangour, T.A., Alsuwayegh, A., Almoqbel, D., Albati, A., Alsaud, A. and Enani, M., 2020. Multidrug-resistant and extensively drug-resistant *Enterobacteriaceae*: prevalence, treatments, and outcomes–a retrospective cohort study. *Infection and Drug Resistance*, 13, pp.4653–4662.

Al-Marzooq, F., Mohd Yusof, M.Y. and Tay, S.T., 2015. Molecular analysis of antibiotic resistance determinants and plasmids in Malaysian isolates of multidrug resistant *Klebsiella pneumoniae*. *PLoS ONE*, 10(7), pp.1–21.

Amador, P., Fernandes, R., Prudêncio, C. and Duarte, I., 2019. Prevalence of antibiotic resistance genes in multidrug-resistant *Enterobacteriaceae* on Portuguese livestock manure. *Antibiotics*, 8(1), p.23.

An, H. C. 2023. *Molecular detection of qnrA and qnrB genes in uropathogenic Escherichia coli (UPEC) isolates from Perak*. Final Year Project. Universiti Tunku Abdul Rahman. Available at: <http://eprints.utar.edu.my/id/eprint/5761> [Accessed 22 March 2024].

Antimicrobial Resistance Collaborators, 2022. Global burden of bacterial antimicrobial resistance in 2019: a systematic analysis. *The Lancet*, 399(10325), pp.629–655.

Blahna, M.T., Zalewski, C., Reuer, J.R., Gunnar Kahlmeter, Foxman, B. and Marrs, C.F., 2006. The role of horizontal gene transfer in the spread of trimethoprim–sulfamethoxazole resistance among uropathogenic *Escherichia coli* in Europe and Canada. *Journal of Antimicrobial Chemotherapy*, 57(4), pp.666–672.

Bodendoerfer, E., Marchesi, M., Imkamp, F., Courvalin, P., Böttger, E.C. and Mancini, S., 2020. Co-occurrence of aminoglycoside and β-lactam resistance mechanisms in aminoglycoside- non-susceptible *Escherichia coli* isolated in the Zurich area, Switzerland. *International Journal of Antimicrobial Agents*, 56(1), pp.1–26.

Brandl, M., Hoffmann, A., Willrich, N., Reuss, A., Reichert, F., Walter, J., Eckmanns, T. and Haller, S., 2021. Bugs that can resist antibiotics but not men: gender-specific differences in notified infections and colonisations in Germany, 2010–2019. *Microorganisms*, 9(5), p.894.

Brolund, A., Sundqvist, M., Kahlmeter, G. and Grape, M., 2010. Molecular characterisation of trimethoprim resistance in *Escherichia coli* and *Klebsiella pneumoniae* during a two year intervention on trimethoprim use. *PLoS ONE*, 5(2), pp.1–5.

Clinical & Laboratory Standards Institute (CLSI), 2011. *Performance Standards for Antimicrobial Susceptibility Testing, 21st Informational Supplement. M100-S21*. [online] Available at: < https://www.researchgate.net/file.PostFileLoader.html?id=59202a0696b7e4d462166956&assetKey=AS%3A496054988533760%401495280134033> [Accessed 24 March 2024].

Clinical & Laboratory Standards Institute (CLSI), 2024. *Performance Standards for Antimicrobial Susceptibility Testing, 34th Informational Supplement. M100:E34:2024*. [online] Available at: < http://em100.edaptivedocs.net/GetDoc.aspx?doc=CLSI%20M100%20ED34:2024&scope=user> [Accessed 24 March 2024].

Cody, V., and Schwalbe, C. H., 2006. Structural characteristics of antifolate dihydrofolate reductase enzyme interactions. *Crystallography Reviews*, 12(4), pp.301–333.

da Silva, K. E., Rossato, L., Leite, A. F., and Simionatto, S., 2022. Overview of polymyxin resistance in *Enterobacteriaceae*. *Revista Da Sociedade Brasileira De Medicina Tropical*, 55, pp.1–5.

Delanaye, P., Mariat, C., Cavalier, E., Maillard, N., Krzesinski, J.M. and White, C.A., 2011. Trimethoprim, creatinine and creatinine-based equations. *Nephron Clinical Practice*, 119(3), pp.187–194.

Di Conza, J.A., Badaracco, A., Ayala, J., Rodriguez, C., Famiglietti, Á. and Gutkind, G.O., 2014. β-lactamases produced by amoxicillin-clavulanate-resistant enterobacteria isolated in Buenos Aires, Argentina: A new blaTEM gene. *Revista Argentina de Microbiología*, 46(3), pp.210–217.

DrugBank, 2022. *Trimethoprim*. [online] Available at: <https://go.drugbank.com/drugs/DB00440> [Accessed 28 March 2023].

Engelking, L.R. ed., 2015. *Textbook of Veterinary Physiological Chemistry*. 2nd ed. Cambridge: Academic Press. pp.93–97.

Fernández-Villa, D., Aguilar, M.R. and Rojo, L., 2019. Folic acid antagonists: antimicrobial and immunomodulating mechanisms and applications. *International Journal of Molecular Sciences*, 20(20), p.4996.

Ferrazzi, E., Tiso, G. and Di Martino, D., 2020. Folic acid versus 5-methyl tetrahydrofolate supplementation in pregnancy. *European Journal of Obstetrics & Gynecology and Reproductive Biology*, 253, pp.312–319.

Goldman, J.L., Leeder, J.S., Van Haandel, L. and Pearce, R.E., 2015. In vitro hepatic oxidative biotransformation of trimethoprim. *Drug Metabolism and Disposition*, 43(9), pp.1372–1380.

Gorelova, V., Ambach, L., Rébeillé, F., Stove, C. and Van Der Straeten, D., 2017. Folates in plants: research advances and progress in crop biofortification. *Frontiers in Chemistry*, 5, pp.1–20.

Grape, M., 2006. *Molecular basis for trimethoprim and sulphonamide resistance in Gram negative pathogens*. [online] Available at: <http://hdl.handle.net/10616/40098> [Accessed 14 Apr. 2024].

Grape, M., Motakefi, A., Pavuluri S.K. and Kahlmeter, G., 2007. Standard and real-time multiplex PCR methods for detection of trimethoprim resistance *dfr* genes in large collections of bacteria. *Clinical Microbiology and Infection*, 13(11), pp.1112–1118.

Hismiogullari, S. E. and Yarsan, E., 2009. Spectrophotometric determination and stability studies of sulfamethoxazole and trimethoprim in oral suspension by classical least square calibration method. *Hacettepe University Journal of the Faculty of Pharmacy*. 29(2), pp. 95–104.

Huovinen, P., 2001. Resistance to Trimethoprim-Sulfamethoxazole. *Clinical Infectious Diseases*, 32(11), pp.1608–1614.

Jafri, S.A., Qasim, M., Masoud, M.S., Rahman, M. -, Izhar, M. and Kazmi, S., 2014. Antibiotic resistance of *E. coli* isolates from urine samples of Urinary Tract Infection (UTI) patients in Pakistan. *Bioinformation*, 10(7), pp.419–422.

Jiang, Y., Peng, K., Wang, Q., Wang, M., Li, R. and Wang, Z., 2023. Novel Trimethoprim resistance gene *dfrA49* identified in *Riemerella anatipestifer* from China. *Microbiology spectrum*, 11(2), pp.1–10.

Jodeh S, Jaber A, Hanbali G, Massad Y, Safi ZS, Radi S, Mehmeti V, Berisha A, Tighadouini S, Dagdag O., 2022. Experimental and theoretical study for removal of trimethoprim from wastewater using organically modified silica with pyrazole-3-carbaldehyde bridged to copper ions. *PubMed Central*, 16(1), pp.1–17.

Kester, M., Karpa, K.D. and Vrana, K.E., 2012. Treatment of Infectious Diseases. In: M. Kester, K. D. Karpa, K. E. Vrana, eds. 2012. *Elsevier's Integrated Review Pharmacology*, United States: W.B. Saunders, pp.41–78.

Kneis, D., Claudèle Lemay-St-Denis, Cellier-Goetghebeur, S., Alan Xavier Elena, Berendonk, T.U., Pelletier, J.N. and Heß, S., 2023. Trimethoprim resistance in surface and wastewater is mediated by contrasting variants of the *dfrB* gene. *The ISME Journal*, 17(9), pp.1455–1466.

Köhler, T., Kok, M., Michea-Hamzehpour, M., Plesiat, P., Gotoh, N., Nishino, T., Curty, L.K. and Pechere, J.C., 1996. Multidrug efflux in intrinsic resistance to trimethoprim and sulfamethoxazole in *Pseudomonas aeruginosa*. *Antimicrobial Agents and Chemotherapy*, 40(10), pp.2288–2290.

Kor, S. B., Choo, Q. C. and Chew, C. H., 2013. New integron gene arrays from multiresistant clinical isolates of members of the *Enterobacteriaceae* and *Pseudomonas aeruginosa* from hospitals in Malaysia. *Journal of Medical Microbiology*, 62(3), pp.412–420.

Kordus, S.L. and Baughn, A.D, 2019. Revitalizing antifolates through understanding mechanisms that govern susceptibility and resistance. *MedChemComm*, 10(6), pp.880–895.

LaPierre, L., Cornejo, J., Asun, A., Vergara, C., Varela, D., 2020. *Laboratory guide: methodologies for antimicrobial susceptibility testing APEC sub-committee on standards and conformance*. [online] Available at: < https://www.apec.org/publications/2020/05/laboratory-guide---methodologies-for-antimicrobial-susceptibility-testing> [Accessed 1 January 2024].

Lee, J.C., Oh, J.Y., Cho, J.W., Park, J.C., Kim, J.M., Seol, S.Y. and Cho, D.T., 2001. The prevalence of trimethoprim-resistance-conferring dihydrofolate reductase genes in urinary isolates of *Escherichia coli* in Korea. *Journal of Antimicrobial Chemotherapy*, 47(5), pp.599–604.

Luterbach, C.L., Boshe, A., Henderson, H.A., Cober, E., Richter, S.S., Salata, R.A., Kalayjian, R.C., Watkins, R.R., Hujer, A.M., Hujer, K.M., Rudin, S.D., T. Nicholas Domitrovic, Doi, Y., Kaye, K.S., Evans, S.R., Fowler, V.G., Bonomo, R.A. and David van Duin, 2018. The role of Trimethoprim/Sulfamethoxazole in the treatment of infections caused by Carbapenem-Resistant *Enterobacteriaceae*. *Open Forum Infectious Diseases*, 6(1), pp.1–3.

Manna, M.S., Tamer, Y.T., Gaszek, I., Poulides, N., Ahmed, A., Wang, X., Toprak, F.C.R., Woodard, D.R., Koh, A.Y., Williams, N.S., Borek, D., Atilgan, A.R., Hulleman, J.D., Atilgan, C., Tambar, U. and Toprak, E., 2021. A trimethoprim derivative impedes antibiotic resistance evolution. *Nature Communications*, 12(1), p.2949.

Marchant, M., Vinué, L., Torres, C. and Moreno, M.A., 2013. Change of integrons over time in *Escherichia coli* isolates recovered from healthy pigs and chickens. *Veterinary Microbiology*, 163(1-2), pp.124–132.

Martijn Sijbom, Büchner, F.L., Saadah, N.H., Numans, M.E. and Mark., 2023. Trends in antibiotic selection pressure generated in primary care and their association with sentinel antimicrobial resistance patterns in Europe. *Journal of Antimicrobial Chemotherapy*, 78(5), pp.1245–1252.

Masters, P.A., O'Bryan, T.A., Zurlo, J., Miller, D.Q. and Joshi, N., 2003. Trimethoprim-sulfamethoxazole revisited. *Archives of internal medicine*, 163(4), pp.402–410.

Matthews, D.A., Bolin, J.T., Burridge, J.M., Filman, D.J., Volz, K.W. and Kraut, J., 1985. Dihydrofolate reductase. The stereochemistry of inhibitor selectivity. *The Journal of Biological Chemistry*, 260(1), pp.392–399.

Mehrishi, P., Faujdar, S.S., Kumar, S., Solanki, S. and Sharma, A., 2019. Antibiotic susceptibility profile of uropathogens in rural population of Himachal Pradesh, India: where we are heading? *Biomedical and Biotechnology Research Journal*, 3(3), p.171.

Ministry of Health Malaysia, 2019. *National antimicrobial guideline 2019*. [online] Available at: <https://pharmacy.moh.gov.my/sites/default/files/document-upload/nag-2019-latest-9-dis-2020_0.pdf > [Accessed 26 March 2023].

Morgan-Linnell, S.K., Boyd, L.B., Steffen, D. and Zechiedrich, L., 2009. Mechanisms accounting for fluoroquinolone resistance in *Escherichia coli* clinical isolates. *Antimicrobial Agents and Chemotherapy*, 53(1), pp.235–241.

National Institute of Diabetes and Digestive and Kidney Diseases, 2020. *Amoxicillin-Clavulanate*. [online] Available at <https://www.ncbi.nlm.nih.gov/books/NBK548517/> [Accessed 17 March 2024].

Navarro-Martínez, M.D., Cabezas-Herrera, J. and Rodríguez-López, J.N., 2006. Antifolates as antimycotics? Connection between the folic acid cycle and the ergosterol biosynthesis pathway in *Candida albicans*. *International Journal of Antimicrobial Agents*, 28(6), pp.560–567.

Organisation for Economic Co-operation and Development, 2024. *Working age population*. [online] Available at: <https://data.oecd.org/pop/elderly-population.htm#indicator-chart> [Accessed 15 March 2024].

Oteo, J., Campos, J., Lázaro, E., Cuevas, Ó., García-Cobos, S., Pérez-Vázquez, M. and de Abajo, F.J., 2008. Increased amoxicillin–clavulanic acid resistance in *Escherichia coli* blood isolates, Spain. *Emerging Infectious Diseases*, 14(8), pp.1259–1262.

Ozma, M. A., Abbasi, A., Asgharzadeh, M., Pagliano, P., Guarino, A., Köse, Ş., and Samadi Kafil, H., 2022. Antibiotic therapy for pan-drug-resistant infections. *Le infezioni in medicina*, 30(4), pp.525–531.

Pérez-Legaspi, I.A. and Rico-Martínez, R., 2023. Antibiotics as contaminants of aquatic ecosystems: antibiotic-resistant genes and antibiotic-resistant bacteria. In: P. Singh, M. Sillanpää, eds. 2023. *Degradation of Antibiotics and Antibiotic-Resistant Bacteria from Various Sources*, Cambridge: Academic Press. pp.143–157.

Poirel, L., Jayol, A. and Nordmann, P., 2017. Polymyxins: antibacterial activity, susceptibility testing, and resistance mechanisms encoded by plasmids or chromosomes. *Clinical Microbiology Reviews*, 30(2), pp.557–596.

Rajpara, N., Kutar, B. M., Sinha, R., Nag, D., Koley, H., Ramamurthy, T., and Bhardwaj, A. K., 2015. Role of integrons, plasmids and SXT elements in multidrug resistance of *Vibrio cholerae* and *Providencia vermicola* obtained from a clinical isolate of diarrhea. *Frontiers in Microbiology*, 6, pp. 1–11.

Reygaert, W.C., 2018. An overview of the antimicrobial resistance mechanisms of bacteria. *AIMS Microbiology*,4(3), pp.482–501.

Rossolini G.M., Arena F., Giani T., 2017. Mechanisms of antibacterial resistance. In: J. Cohen, W. G. Powderly, S. M. Opal, eds. 2017. *Infectious Diseases*. Amsterdam: Elsevier. pp. 1181–1196.

Rowan-Nash, A. D., Araos, R., D'Agata, E. M. C., and Belenky, P., 2020. Antimicrobial resistance gene prevalence in a population of patients with advanced dementia is related to specific pathobionts. *iScience*, 23(3), pp.1–33.

Sánchez-Osuna, M., Cortés, P., Llagostera, M., Barbé, J. and Erill, I., 2020. Exploration into the origins and mobilization of di-hydrofolate reductase genes and the emergence of clinical resistance to trimethoprim. *Microbial Genomics*, 6(11), pp.1–13.

Sandalli, C., Buruk, C.K., Sancaktar, M. and Ozgumus, O.B., 2009. Prevalence of integrons and a new *dfrA17* variant in Gram-negative bacilli which cause community-acquired infections. *Microbiology and Immunology*, 54(3), pp.164–169.

Šeputienė, V., Povilonis, J., Ružauskas, M., Pavilonis, A. and Sužiedėlienė, E., 2010. Prevalence of trimethoprim resistance genes in *Escherichia coli* isolates of human and animal origin in Lithuania. *Journal of Medical Microbiology*, 59(3), pp.315–322.

Sigma Aldrich, 2021. *TAE and TBE Running Buffers Recipe & Video*. [online] Available at: <https://www.sigmaaldrich.com/MY/en/technical-documents/protocol/protein-biology/gel-electrophoresis/tae-and-tbe-running-buffers-recipe> [Accessed 24 December 2023].

Somorin, Y.M., Weir, N.-J.M., Pattison, S.H., Crockard, M.A., Hughes, C.M., Tunney, M.M. and Gilpin, D.F., 2022. Antimicrobial resistance in urinary pathogens and culture-independent detection of trimethoprim resistance in urine from patients with urinary tract infection. *BMC Microbiology*, 22(1), pp.1–8.

Teng, C. L., Tong, S. F., Khoo, E. M., Lee, V., Zailinawati, A. H., Mimi, O., Chen, W. S. and Nordin, S., 2011. Antibiotics for URTI and UTI: Prescribing in Malaysian primary care settings. *Australian Family Physician*, 40(5), pp.325–329.

van der Veen, E. L., Schilder, A. G. M., Timmers, T. K., Rovers, M. M., Fluit, A. C., Bonten, M. J., Leverstein-van Hall, M. A., 2009. Effect of long-term trimethoprim/sulfamethoxazole treatment on resistance and integron prevalence in the intestinal flora: a randomized, double-blind, placebo-controlled trial in children. *Journal of Antimicrobial Chemotherapy*, 63(5), pp.1011–1016.

van Hoek, A.H.A.M., Mevius, D., Guerra, B., Mullany, P., Roberts, A.P. and Aarts, H.J.M., 2011. Acquired antibiotic resistance genes: an overview. *Frontiers in Microbiology*, 2(203), pp.1–27.

Wang, S., Zhao, S., Zhou, Y., Jin, S., Ye, T. and Pan, X., 2023. Antibiotic resistance spectrum of *E. coli* strains from different samples and age-grouped patients: a 10-year retrospective study. *BMJ Open*, 13(4), pp.1–8.

White, P.A., McIver, C.J. and Rawlinson, W.D., 2001. Integrons and gene cassettes in the *Enterobacteriaceae*. *Antimicrobial Agents and Chemotherapy*, 45(9), pp.2658–2661.

Wróbel, A., Arciszewska, K., Maliszewski, D. and Drozdowska, D., 2019. Trimethoprim and other nonclassical antifolates an excellent template for searching modifications of dihydrofolate reductase enzyme inhibitors. *The Journal of Antibiotics*, 73(1), pp.5–27.

Wu, L., Xie, X., Li, Y., Liang, T., Zhong, H., Ma, J., Yang, L., Yang, J., Li, L., Xi, Y., Li, H., Zhang, J., Chen, X., Ding, Y., and Wu, Q., 2021. Metagenomics-based analysis of the age-related cumulative effect of antibiotic resistance genes in gut microbiota. *Antibiotics*, 10(8), p.1–16.

Yadav, K.K., Adhikari, N., Khadka, R., Pant, A.D. and Shah, B., 2015. Multidrug resistant *Enterobacteriaceae* and extended spectrum β-lactamase producing *Escherichia coli*: a cross-sectional study in National Kidney Center, Nepal. *Antimicrobial Resistance and Infection Control*, 4(1), pp.1–7.

Yekani, M., Baghi, H.B., Sefidan, F.Y., Azargun, R., Memar, M.Y. and Ghotaslou, R., 2018. The rates of quinolone, trimethoprim/sulfamethoxazole and aminoglycoside resistance among *Enterobacteriaceae* isolated from urinary tract infections in Azerbaijan, Iran. *GMS Hygiene and Infection Control*, 13, pp.1–6.

Yu, H.S., 2004. Prevalence of *dfr* genes associated with integrons and dissemination of *dfrA17* among urinary isolates of *Escherichia coli* in Korea. *Journal of Antimicrobial Chemotherapy*, 53(3), pp.445–450.

Zheng, Y. and Cantley, L.C., 2018. Toward a better understanding of folate metabolism in health and disease. *Journal of Experimental Medicine*, 216(2), pp.253–266.

Zinner, S. and Mayer, K., 2015. *Sulfonamides and Trimethoprim*. [online] Available at: <https://doi.org/10.1016/B978-1-4557-4801-3.00033-3> [Accessed 7 January 2024].

APPENDICES

Appendix A

Table 1: Demographic data of the clinical isolates used.

Species	Sample	Types of specimens	Gender	Age
Escherichia coli	A7	Blood	M	79
Enterobacter cloacae	G21	Swab	M	58
Morganella morganii	G52	Swab foot	F	62
Citrobacter freundii	G63	Pus swab	M	38
Enterobacter aerogenes	G66	left ear swab	M	53
Enterobacter cloacae	G69	Mucoid sputum	M	61
Escherichia coli	G7	Swab	M	46
Escherichia coli	H12	Pus swab	F	21
Klebsiella pneumoniae	H14	Endotracheal tube aspirate	F	7
Klebsiella pneumoniae	H15	Pus swab	F	56
Klebsiella pneumoniae	H16	Urine	F	27
Klebsiella pneumoniae	H19	Pus swab	M	79
Escherichia coli	H21	Pus swab	F	69
Klebsiella pneumoniae	H22	Endotracheal tube aspirate	M	79
Enterobacter amnigenus	H23	Endotracheal tube aspirate	M	79
Klebsiella pneumoniae	H26	Bone cls	M	60
Klebsiella pneumoniae	H27	Swab cls	M	60
Klebsiella pneumoniae	H28	Urine	M	53
Escherichia coli	H3	Umbilical Venous catheters tip	M	new-born
Klebsiella pneumoniae	H31	Urine	M	25
Klebsiella pneumoniae	H32	Tissue	M	60
Escherichia coli	H33	Pus swab	M	29
Klebsiella pneumoniae	H34	Trachy aspirate	F	75
Escherichia coli	H35	Urine	M	49
Klebsiella pneumoniae	H38	Tissue	M	67
Klebsiella pneumoniae	H4	Urine	F	88
Klebsiella pneumoniae	H40	Blood	F	2
Escherichia coli	H41	Pus swab	F	75
Klebsiella pneumoniae	H43	Sputum	F	61
Klebsiella pneumoniae	H45	Urine	F	0

Table 1 (continue):

Enterobacter cloacae	H5	Pus swab	M	49
Escherichia coli	H52	Blood	M	48
Escherichia coli	H54	Urine	M	5
Klebsiella pneumoniae	H55	Trachy aspirate	F	12
Klebsiella pneumoniae	H56	Pus swab	M	46
Klebsiella pneumonia	H57	Pus swab	M	68
Klebsiella pneumonia	H58	Pus swab	F	51
Escherichia coli	H59	Pus swab	M	68
Klebsiella pneumonia	H6	Urine	F	59
Klebsiella pneumonia	H62	Pus swab	M	62
Klebsiella pneumonia	H63	Urine	M	53
Klebsiella pneumonia	H65	Urine	F	21
Klebsiella pneumonia	H66	Pus swab	M	66
Klebsiella pneumonia	H67	Tissue	M	55
Klebsiella pneumonia	H68	Urine	M	80
Klebsiella pneumonia	H71	Blood	F	50
Klebsiella pneumonia	H73	Endotracheal tube aspirate	M	63
Escherichia coli	H8	Pus swab	M	70
Escherichia coli	H9	Pus swab	F	78
Escherichia coli	K16	Urine	F	60
Klebsiella pneumonia	K21	Sputum	F	77
Escherichia coli	K3	Urine	F	16
klebsiella pneumoniae	P1	Urine	F	77
Escherichia coli	P4	High vaginal swab	F	49
Escherichia coli	P8	Urine	F	56
Pseudomonas aeruginosa	A6	sputum	F	79
Pseudomonas aeruginosa	K18	Tracheal aspirate	M	20
Pseudomonas aeruginosa	K2	Wound swab	M	81
Pseudomonas aeruginosa	K25	ETT secretion	M	72
Pseudomonas aeruginosa	K5	Swab from left ear	M	79

Appendix B

Table 2: The interpretative categories and zone diameter breakpoint (to the nearest whole mm) for *Enterobacterales* as provided by CLSI guidelines (2024).

Antibiotics	Amoxicillin-clavulanic acid (20/10 µg)	Ciprofloxacin (5 µg)	Nalidixic acid (30 µg)	Netillin (30 µg)	Polymyxin B	Tobramycin (10 µg)	TMP-SMZ (1.25/ 23.75 µg)
Susceptible	≥18	≥26	≥19	≥15	≥12[a]	≥17	≥16
Intermediate	14–17	22–25	14–18	13–14	9–11[a]	13–16	11–15
Resistant	≤13	≤21	≤13	≤ 12	≤8[a]	≤12	≤10

[a]The subscripts letter represent the breakpoints and interpretative categories adapted from (Al-Ajmi, Rahman and Banu, 2020).

Table 3: The interpretative categories and zone diameter breakpoint (to the nearest whole mm) for *Pseudomonas aeruginosa* as provided by CLSI guidelines (2024).

Antibiotics	Amoxicillin-clavulanic acid (20/10 µg)	Ciprofloxacin (5 µg)	Nalidixic acid (30 µg)	Netillin (30 µg)	Polymyxin B	Tobramycin (10 µg)	TMP-SMZ (1.25/ 23.75 µg)
Susceptible	≥18[c]	≥25	≥15[b]	≥15	≥12[b]	≥19	≥16
Intermediate	14–17[c]	19–24	-[b]	13–14	-[b]	13–18	11–15
Resistant	≤13[c]	≤18	≤12[b]	≤12	≤11[b]	≤12	≤10

[b]The subscripts letter represent the interpretative breakpoinsts adapted from CLSI (2011).
[c]The subscripts letter represent the interpretative breakpoinsts adapted from Mehrishi, et al. (2019).

Appendix C

Table 4: Concentration and the purity ratio (A260/A280) of extracted DNA.

Species	Sample	Nucleic acid concentration (ng/µL)	A260/A280 ratio
Escherichia coli	A7	323.5	2.00
Enterobacter cloacae	G21	802.3	1.96
Morganella morganii	G52	330.0	1.75
Citrobacter freundii	G63	1441.5	1.97
Enterobacter aerogenes	G66	543.9	2.00
Enterobacter cloacae	G69	933.1	1.92
Escherichia coli	G7	193.5	1.81
Escherichia coli	H12	674.9	1.88
Klebsiella pneumoniae	H14	657.1	1.97
Klebsiella pneumoniae	H15	238.4	2.01
Klebsiella pneumoniae	H16	165.1	1.83
Klebsiella pneumoniae	H19	1836.8	1.86
Escherichia coli	H21	603.6	2.00
Klebsiella pneumoniae	H22	1835.5	1.93
Enterobacter amnigenus	H23	798.4	1.73
Klebsiella pneumoniae	H26	1890.2	1.91
Klebsiella pneumoniae	H27	363.5	1.81
Klebsiella pneumoniae	H28	147.7	1.97
Escherichia coli	H3	246.9	1.77
Klebsiella pneumoniae	H31	563.4	1.95
Klebsiella pneumoniae	H32	496.6	1.90
Escherichia coli	H33	729.7	1.87
Klebsiella pneumoniae	H34	587.6	1.83
Escherichia coli	H35	205	1.89
Klebsiella pneumoniae	H38	649.6	1.80
Klebsiella pneumoniae	H4	940	1.92
Klebsiella pneumoniae	H40	1859.7	1.83
Escherichia coli	H41	1372.9	1.99
Klebsiella pneumoniae	H43	805.4	1.90
Klebsiella pneumoniae	H45	919.8	1.94
Enterobacter cloacae	H5	738.1	1.95
Escherichia coli	H52	999.6	1.92
Escherichia coli	H54	417.8	1.93
Klebsiella pneumoniae	H55	758.9	1.80

Table 4 (continue):

Klebsiella pneumoniae	H56	257.5	1.83
Klebsiella pneumonia	H57	687.4	2.03
Klebsiella pneumonia	H58	480.8	1.84
Escherichia coli	H59	804.3	1.96
Klebsiella pneumonia	H6	553.3	1.83
Klebsiella pneumonia	H62	819	1.98
Klebsiella pneumonia	H63	624.7	1.89
Klebsiella pneumonia	H65	590.1	1.82
Klebsiella pneumonia	H66	1327.7	1.88
Klebsiella pneumonia	H67	1143.5	1.92
Klebsiella pneumonia	H68	240.8	1.84
Klebsiella pneumonia	H71	133.5	1.49
Klebsiella pneumonia	H73	506.9	1.50
Escherichia coli	H8	849.1	1.94
Escherichia coli	H9	380.8	1.68
Escherichia coli	K16	584.6	1.87
Klebsiella pneumonia	K21	236.6	1.90
Escherichia coli	K3	183.5	1.92
klebsiella pneumoniae	P1	315.7	1.86
Escherichia coli	P4	360.8	1.89
Escherichia coli	P8	425.3	1.83
Pseudomonas aeruginosa	A6	341.9	1.85
Pseudomonas aeruginosa	K18	127.5	1.57
Pseudomonas aeruginosa	K2	374.4	1.89
Pseudomonas aeruginosa	K25	171.9	1.49
Pseudomonas aeruginosa	K5	325.6	1.64

Appendix D

Table 5: Representative statistical analysis of negative association (association between gender and *dfrA1* gene prevalence).

dfrA1 * Gender Crosstabulation

			Gender		
			Male	Female	Total
dfrA1	Presence	Count	5	3	8
		Expected Count	4.8	3.2	8.0
		% within dfrA1	62.5%	37.5%	100.0%
		% within Gender	13.9%	12.5%	13.3%
		% of Total	8.3%	5.0%	13.3%
	Absence	Count	31	21	52
		Expected Count	31.2	20.8	52.0
		% within dfrA1	59.6%	40.4%	100.0%
		% within Gender	86.1%	87.5%	86.7%
		% of Total	51.7%	35.0%	86.7%
Total		Count	36	24	60
		Expected Count	36.0	24.0	60.0
		% within dfrA1	60.0%	40.0%	100.0%
		% within Gender	100.0%	100.0%	100.0%
		% of Total	60.0%	40.0%	100.0%

Chi-Square Tests

	Value	df	Asymptotic Significance (2-sided)	Exact Sig. (2-sided)	Exact Sig. (1-sided)
Pearson Chi-Square	.024[a]	1	.877		
Continuity Correction[b]	.000	1	1.000		
Likelihood Ratio	.024	1	.876		
Fisher's Exact Test				1.000	.598
Linear-by-Linear Association	.024	1	.878		
N of Valid Cases	60				

a. 2 cells (50.0%) have expected count less than 5. The minimum expected count is 3.20.

b. Computed only for a 2x2 table

Symmetric Measures

		Value	Approximate Significance
Nominal by Nominal	Phi	.020	.877
	Cramer's V	.020	.877
N of Valid Cases		60	

Table 6: Representative statistical analysis of negative association (association between gender and *dfrA7* gene prevalence).

dfrA7 * Gender Crosstabulation

			Gender		
			Male	Female	Total
dfrA7	Absence	Count	29	22	51
		Expected Count	30.6	20.4	51.0
		% within dfrA7	56.9%	43.1%	100.0%
		% within Gender	80.6%	91.7%	85.0%
		% of Total	48.3%	36.7%	85.0%
	Presence	Count	7	2	9
		Expected Count	5.4	3.6	9.0
		% within dfrA7	77.8%	22.2%	100.0%
		% within Gender	19.4%	8.3%	15.0%
		% of Total	11.7%	3.3%	15.0%
Total		Count	36	24	60
		Expected Count	36.0	24.0	60.0
		% within dfrA7	60.0%	40.0%	100.0%
		% within Gender	100.0%	100.0%	100.0%
		% of Total	60.0%	40.0%	100.0%

Chi-Square Tests

	Value	df	Asymptotic Significance (2-sided)	Exact Sig. (2-sided)	Exact Sig. (1-sided)
Pearson Chi-Square	1.394[a]	1	.238		
Continuity Correction[b]	.659	1	.417		
Likelihood Ratio	1.490	1	.222		
Fisher's Exact Test				.293	.211
Linear-by-Linear Association	1.371	1	.242		
N of Valid Cases	60				

a. 1 cells (25.0%) have expected count less than 5. The minimum expected count is 3.60.

b. Computed only for a 2x2 table

Symmetric Measures

		Value	Approximate Significance
Nominal by Nominal	Phi	-.152	.238
	Cramer's V	.152	.238
N of Valid Cases		60	

Appendix E

Table 7: Representative data of statistical analysis on the negative association between *dfrA1* gene and trimethoprim-sulfamethoxazole resistance profile.

Crosstab

			dfrA1		
			Presence	Absence	Total
SXT	Resistant	Count	8	34	42
		Expected Count	5.6	36.4	42.0
		% within SXT	19.0%	81.0%	100.0%
		% within dfrA1	100.0%	65.4%	70.0%
		% of Total	13.3%	56.7%	70.0%
	Susceptible	Count	0	18	18
		Expected Count	2.4	15.6	18.0
		% within SXT	0.0%	100.0%	100.0%
		% within dfrA1	0.0%	34.6%	30.0%
		% of Total	0.0%	30.0%	30.0%
Total		Count	8	52	60
		Expected Count	8.0	52.0	60.0
		% within SXT	13.3%	86.7%	100.0%
		% within dfrA1	100.0%	100.0%	100.0%
		% of Total	13.3%	86.7%	100.0%

Chi-Square Tests

	Value	df	Asymptotic Significance (2-sided)	Exact Sig. (2-sided)	Exact Sig. (1-sided)
Pearson Chi-Square	3.956[a]	1	.047		
Continuity Correction[b]	2.479	1	.115		
Likelihood Ratio	6.220	1	.013		
Fisher's Exact Test				.091	.046
Linear-by-Linear Association	3.890	1	.049		
N of Valid Cases	60				

a. 1 cells (25.0%) have expected count less than 5. The minimum expected count is 2.40.

b. Computed only for a 2x2 table

Symmetric Measures

		Value	Approximate Significance
Nominal by Nominal	Phi	.257	.047
	Cramer's V	.257	.047
N of Valid Cases		60	

Table 8: Representative data of statistical analysis on the positive association between *dfrA7* gene and trimethoprim-sulfamethoxazole resistance profile.

Crosstab

			dfrA7		
			Absence	Presence	Total
SXT	Resistant	Count	33	9	42
		Expected Count	35.7	6.3	42.0
		% within SXT	78.6%	21.4%	100.0%
		% within dfrA7	64.7%	100.0%	70.0%
		% of Total	55.0%	15.0%	70.0%
	Susceptible	Count	18	0	18
		Expected Count	15.3	2.7	18.0
		% within SXT	100.0%	0.0%	100.0%
		% within dfrA7	35.3%	0.0%	30.0%
		% of Total	30.0%	0.0%	30.0%
Total		Count	51	9	60
		Expected Count	51.0	9.0	60.0
		% within SXT	85.0%	15.0%	100.0%
		% within dfrA7	100.0%	100.0%	100.0%
		% of Total	85.0%	15.0%	100.0%

Chi-Square Tests

	Value	df	Asymptotic Significance (2-sided)	Exact Sig. (2-sided)	Exact Sig. (1-sided)
Pearson Chi-Square	4.538[a]	1	.033		
Continuity Correction[b]	3.013	1	.083		
Likelihood Ratio	7.080	1	.008		
Fisher's Exact Test				.047	.030
Linear-by-Linear Association	4.462	1	.035		
N of Valid Cases	60				

a. 1 cells (25.0%) have expected count less than 5. The minimum expected count is 2.70.

b. Computed only for a 2x2 table

Symmetric Measures

		Value	Approximate Significance
Nominal by Nominal	Phi	-.275	.033
	Cramer's V	.275	.033
N of Valid Cases		60	